The primoridal origin of Jupiter mass Binary Objects

Simon F. Portegies Zwart,
Erwan Hochart

Leiden Observatory, Leiden University, PO Box 9513, 2300 RA, Leiden, The Netherlands
* spz@strw.leidenuniv.nl

Abstract

The recently observed population of 540 free-floating jupiter-mass objects, and 42 dynamically soft pairs of jupiter-mass planets, among which 2 with a tertiary companion, in the Trapezium cluster has raised interesting questions on their formation and further evolution. We test various scenarios for the origin and survivability of these free floating jupiter-mass planets and Jupiter-mass Binary Objects (JuMBOs) in the Trapezium cluster. The numerical calculations are performed by direct N-body integration of the stars and planets in the Trapezium cluster starting with a wide variety of planets in various configurations. We discuss four main models: $\mathcal{SPP}$ in which selected stars have two outer orbiting jupiter-mass planets; $\mathcal{SPM}$ where selected stars are orbited by jupiter-mass planet-moon pairs; $\mathcal{ISF}$ in which JuMBOs form in situ together with the stars, and $\mathcal{FFC}$ where we introduce a population of free floating single jupiter-mass objects, but no binaries. Models $\mathcal{SPP}$ and $\mathcal{FFC}$ spectacularly fail to produce enough JuMBOs. Models $\mathcal{SPM}$ can produce sufficient free floaters and JuMBOs but require to start with unrealistically wide orbits for the planet-moon system around the star. The observations are best explained with in situ formation (model $\mathcal{ISF}$) of JuMBOs. The observed populations of JuMBOs and free floating planets in the Trapezium cluster are best reproduced if they formed in pairs and as free floaters together with the other stars in a smooth (Plummer) density profile with a virial radius of ~ 0.5 pc. A fractal (with fractal dimension 1.6) stellar density distribution works also, but requires a very high initial binary fraction (close to unity) among free floating planet-mass objects. This would make the primordial binary fraction of jumbos even higher than the already high observed fraction of ~ 8 % (42/540). The fraction of JuMBOs will continue to drop with time, and the lack of jumbos in Upper Scorpius could then result of its higher age, causing more JuMBOs to be ionized. We then also predict that the interstellar density of jupiter-mass objects (either single or some lucky surviving binaries) is ~ 0.05 JuMBOs per pc^{-3} (or around 0.24 per star).

1 Introduction

Recently [1] reported on the discovery of 42 Jupiter-Mass Binary Objects (JuMBOs) in the direction of the Trapezium cluster. Their component masses range between $0.6\,M_{\rm Jup}$ and $14\,M_{\rm Jup}$ and have projected separations between 25 au and 380 au. Two of these objects have a nearby tertiary jupiter-mass companion. They also observed a population of 540 single objects in the same mass range. This discovery initiates the discussions on the origin and surviveability of weakly bound jupiter-mass pairs in a clustered environment.

The first single free-floating jupiter-mass objects have been found in the direction of the Trapzium cluster more than 20 years ago [2–4]. Many more have been found since then, for example in the young clustered environment of Upper Scorpio [5], and through gravitational microlensing surveys in the direction of the Galactic bulge [6]. Their abundance may be as high as $1.9^{+1.3}_{-0.8}$ per star [6], although a considerable fraction of these could be in wide orbits.

The origin of these free floating planets has been actively debated [7]. Star formation, from the collapse of a molecular cloud through gravitational instability, generally is expected to lead to objects considerably more massive than Jupiter [8, 9], and in disks planets tend to form with masses. As a consequence, the large population of jupiter-mass free-floaters is often considered to result from fully packed planetary systems [10], or kicked out of their orbit by encounters with other stars in the young cluster [11]. Single jupiter-mass free floating objects then originally formed in a disk around a star but became single later in life [11–16]. The number of super-jupiter mass free floating planets formed in this way is expected to be on the order of one (~ 0.71) per star [11], but lower-mass free floaters orphaned this way may be much more abundant [14]; The origin of relatively massive free-floaters through dynamical phenomena is further complicated by the tendency for lower mass planets to be more prone to ejections [16–19].

Explaining the observed abundance and mass-function of single free-floating jupiter-mass objects is difficult. In particular the large population of objects in Upper Scorpio challenges the formation channels. With the new discovery of a large population of of paired free floaters complicates matters even further, and puts strong constraints about their origin. So far, binary free-floaing planet-mass object have been rare, and were only discovered in tight (few au) orbits [20]. Known interstellar jupiter-mass binary objects include only four objects:

- 2MASS J11193254-1137466 AB: a 5 to 10 $M_{\rm Jup}$ primary in a $a = 3.6 \pm 0.9$ au orbit [21].
- WISE 1828+2650: a 3 to 6$M_{\rm Jup}$ primary with a 5 $M_{\rm Jup}$ companion in an $\gtrsim 0.5$ au orbit [22].
- WISE J0336-014: a 8.5 to 18 $M_{\rm Jup}$ primary with a 5 to 11.5 $M_{\rm Jup}$ companion in a $0.9^{+0.05}_{-0.09}$ au orbit [23].
- 2MASS J0013-1143 discovered by [24] and suspected to be a binary by [25].

Such tight pairs could have formed as binary planets (or planet-moon pairs) orbiting a stars, to be dislodged from their parents to become JuMBOs [26]. So long only a few were discovered such an exotic scenario seems to pose a reasonable explanation for their existence, but the discovery of a rich population of 42 wide JuMBOs [1] requires a more thorough study on their origin.

Adopting a dynamical origin, or at least a dynamical history, we perform direct N-body simulations of a Trapezium-like star cluster with primordial Jupiter-mass objects (JMO) and JuMBOs. Our simulations focus on four models that could explain the abundance, their masses, and the orbital characteristics (actually the observed separation distribution) of the observed jupiter-mass objects in the cluster. In this paper, we perform a rudimentary analysis on four scenarios capable of forming JuMBOs. Alternative to forming in situ (scenario $\mathcal{ISF}$), one can naively imagine three mechanisms to form JuMBOs. [27] argued that these binaries could be explained from hierarchical planetary systems of which the outer two planets are stripped by a passing star in a close encounter. The two ejected planets would lead to a population of free floating planets, but could also explain the observed population of JuMBOs. We call this scenario $\mathcal{SPP}$ (for star planet-planet).

Alternatively one could imagine JuMBOs to result from planet-moon pairs (or binary planets) orbiting some star that is ejected to become a JuMBO. We call this scenario $\mathcal{SPM}$, for star planet-moon.

Finally, one could imagine that a sufficiently large population of free-floating jupiter-mass objects could lead to a population of JuMBOs by dynamical capture of one JMO by another. We call this scenario $\mathcal{FFC}$ (free floating capture). A similar scenario was proposed by [28] for explaining very wide stellar pairs, but the model was also adopted to account for wide planetary orbits [29,30]

We start by discussing some fundamental properties of the environmental dynamics, followed by a description of models, the numerical simulations to characterize the parameters of the acquired JuMBOs, and the resulting occurrence rates.

2 The dynamical characterization of JuMBOs

The JuMBOs discovered by [1] were located in the Trapezium cluster. We base our analysis on the parameters derived for this cluster by [31] by numerical modeling of disk-size distributions observed in the Trapezium cluster, and concluded that this distribution is best reproduced for a cluster containing ~ 2500 stars with a total mass of $\sim 900\,M_\odot$ and a half-mass radius of ~ 0.5 pc. The results were inconsistent with a Plummer [32] distribution, but match the observations if the initial cluster density distribution represented a fractal dimension of 1.6. Nevertheless, for consistency with earlier studies, we perform our analysis for Plummer as well as for a fractal (with fractal dimension 1.6) distributions.

Adopting a Plummer distribution of the Trapezium cluster (with $r_{\rm vir} = 0.5$ pc virial radius), the cluster core radius $r_c \simeq 0.64 r_{\rm vir} \sim 0.32$ pc with a core mass of $250\,M_\odot$, resulting in a velocity dispersion of $v_{\rm disp} \equiv GM/\sqrt{r_c^2 + r_{\rm vir}^2} \simeq 0.97$ km/s. With a mean stellar mass in the cluster core of $1\,M_\odot$ the unit of energy expressed in the kinematic temperature kT becomes $\sim 8 \cdot 10^{42}$ erg.

Jumbos are found in the mass range of about $0.6\,M_{\rm Jup}$ to $14\,M_{\rm Jup}$ and have a projected separation of 25 au and $\sim$ 380 au. The averaged observed values are $d = 200 \pm 109$ au, $\langle M \rangle = 4.73 \pm 3.48\,M_{\rm Jup}$, and $\langle m \rangle = 2.81 \pm 2.29\,M_{\rm Jup}$. The median and 25 % to 75 % percentiles are $d = 193.8^{+78.2}_{-114.1}$ au $M = 3.67^{+1.31}_{-1.57}\,M_{\rm Jup}$, and $m = 2.10^{+1.05}_{-1.05}\,M_{\rm Jup}$.

To simplify our analysis, let us assume that the observed variation in projected distances between the two Jupiter-mass objects corresponds to an orbital separation, and express distances in terms of semi-major axis (see Appendix A for motivation). In practice, the differences between the projected separation and the actual semi-major axis of the orbit is small. Adopting a statistical approach, a thermal distribution in eccentricities and a random projection on the sky, the semi-major axis is statitically ~ 1.2 times the projected separation. For the observed JuMBOs we do not really know if they are bound, and if so, we do not know the underlying eccentricity distribution, but in practice this difference between projected separation and actual semi-major axis of a bound population is negligible compared to the 25% to 75% uncertainty intervals derived with the simulations.

To first order, the binding energy of jumbos then ranges between $\sim 5{\cdot}10^{37}$ erg and $1.4{\cdot}10^{41}$ erg, or at most ~ 0.02 kT. This makes them soft upon an encounter with a cluster star.

The hardest JuMBO, composed of two $14\,M_{\rm Jup}$ planets in a 25 au orbit would be hard for another encountering object of less then $17\,M_{\rm Jupiter}$. For an encountering $1\,M_{\rm Jup}$ object a 25 au orbit would be hard only if the two planets are about three times as massive a Jupiter. This entails that JuMBOs are often soft for any encountering free floating giant planet unless they are in tight enough orbits or the perturber is of low mass. On average, soft encounters tend to soften these binaries even further [33], although an occasional soft encounter with another planet may actually slightly harden the JuMBO. Independent of how tight the orbit, JuMBOs are expected to be relatively short lived, because they easily dissociate upon a close encounter with any other cluster member. Once ionized they contribute to the population of free floating single objects. Note that in the Trapezium cluster, even the orbits of 2MASS J11193254-1137466AB, and WISE 1828+2650 would be soft ($\gtrsim 0.025$ kT); they could have been the hardest survivors of an underlying population.

To further understand the dynamics of JuMBOs in a clustered environment, and to study the efficiency of the various formation scenarios we perform direct N-body calculations of the Trapezium star cluster with a population of jupiter-mass objects in various initial configurations.

3 Model calculations

For each of our proposed models, $\mathcal{ISF}$ (in situ formation of jumbos), $\mathcal{SPP}$ (JuMBOs formed via ejections of a host stars outer planets), $\mathcal{SPM}$ (as planet-moon pairs orbiting a star), and $\mathcal{FFC}$ (as mutual capture of free-floaters) we perform a series of N-body simulations with properties consistent with the Trapezium cluster.

Each cluster starts with 2500 single stars taken from a broken power-law mass-function [34] between 0.08 $M_\odot$ and 30 $M_\odot$ distributed either in a Plummer sphere (model Pl) or a fractal distribution with a fractal dimension of 1.6 (model Fr). All models start in virial equilibrium. We run three models for each set of initial conditions, with a virial radius of 0.25 pc, 0.5 pc and 1.0 pc, called model R025, R05 and R100, respectively. We further assume stellar radii to follow the zero-age main sequence, and the radius of jupiter-mass objects based on a density consistent with Jupiter ($\sim$ 1.33 g/cc).

For each of our proposed models, we initialize a population of single JMOs and/or JuMBOs (binary JMOs). The single (and primaries in planet pairs) are selected from a power-law mass function between 0.8 $M_{\rm Jup}$ and 14 $M_{\rm Jup}$, which is consistent with the observed mass function [1]. We fitted a power-law to the primary-planet mass function, which has a slope of $\alpha_{\rm JuMBO} = -1.2$ (considearbly flatter than Salpter's $\alpha_{\rm Salpter} = -2.35$).

This relatively flat mass function is not inconsistent with the mass distribution of earlier observed free floaters The first dozen discovered free floaters already seemd to have a rather flat mass function [3], but the large statistics available through gravitational microlensing surveys allowd a reliable estimate of the slope, which yields $\alpha = -1.3^{+0.3}_{-0.4}$ [6]. This mass function is somewhat steeper than the slope derived for lower-mass free floaters ($\alpha = -0.96^{+0.47}_{-0.27}$ [35]).

For each of the four models, we have a special set of initial configurations. The clusters all have the same statistical representation, being either Plummer or fractal density distributions, virialized and with a virial radius of 0.25 ,pc, 0.5 pc and 1.0 pc. But the distribution of JMOs and JuMBOs varies per model. In figure 3.4 we scetsch the various models.

3.1 Model $\mathcal{SPP}$: Star hierarchically orbited by two planets

For scenario $\mathcal{SPP}$, we selected the star to host such a planetary system from the 150 stars lower in mass than 0.6 $M_\odot$ and 150 more massive stars. The mid-mass point (of 0.6 $M_\odot$) is almost twice the mean stellar mass in the mass function.

We select the same planet masses as for the primordial JuMBOs except that we have them orbiting one of the selected stars as a hierarchical planetary system. The distance from the first planet a_1 and the second planet a_2 (such that $a_2 > a_1$) are selected according to various criteria. The inner orbit a_1 was selected randomly between 25 au and 400 au from a flat distribution in a. The outer orbit, a_2, we typically chose to be five times larger than the inner planet's Hill radius. This guarantees that the planetary systems would be rather stable when in isolation, but they are still rather vulnerable for external perturbations.

Both planetary orbits are rather circular with a random eccentricity from the thermal distribution between circular and 0.02. The mass of the secondary planet (could be either the inner one or the outer one) was selected randomly from a thermal distribution between a mass ratio of 0.2 and unity. As a consequence, we have a slight preference for planets of comparable mass, and we do have a population of $\lesssim 0.8\,M_{\rm Jup}$ objects, which are not observed. This low-mass population contributes to $\sim$ 7.3 % of the total.

The two planets orbit the star in a plane with a relative inclination randomly between -1° and 1°. The other orbital elements are randomly taken from their isotripic distributions.

We perform an additional series of simulations with pre-specified orbital separations for the two planets a_1 and a_2, to follow the model proposed in [27]. The results of these runs are presented in figure 2.

3.2 Model $\mathcal{SPM}$: Star orbited by a pair of planet-mass objects

In the $\mathcal{SPM}$ models we initialize planet pairs (or planet with moons) in orbit around a star. The masses of the stars, planets and moons are selected as in the $\mathcal{SPP}$ model. The planet-moon system orbit was selected from a flat distribution in a between 25 au and 200 au, and with a eccentricity from the thermal distribution with a maximum of 0.02 for the planet-moon orbit.

To warrant stability of the star-planet-moon system, we chose an orbital separation such that the planet-moon pair stays witin 1/3th of it's Hill radius in orbit around the star, again with an eccentricity smaller than 0.02 taken randomly from the thermal distribution.

The planet-moon system is randomly orientation at a distance from the star such that the planet-moon's orbital separation is one-third of it's Hill radius. This guarantees a stable planet-moon pair in orbit around the selected star, but their orbits tend to be rather wide. two jupiter-mass objects in a circular 100 au orbit around a 1 $M_\odot$ star would lead to a circum-stellar orbit of about 3488 au. The orbital elements for the planet-moon system around the star is subseqenly isotropically randomized.

3.3 Model $\mathcal{ISF}$: Jupiter-mass objects in weakly bound orbits

Primordial JuMBOs (model $\mathcal{ISF}$) are initialized with semi-major axis with a flat distribution between 25 au and 1000 au (in some cases 10^4 au), an eccentricity from the thermal distribution between 0 and 1, but they are to remain separated at pericenter. The masses are selected as in model $\mathcal{SPP}$. Each is subsequently rotated to a random orientation. The binaries are subsequently sprinkled in the cluster potential as single objects using the same initial distribution function as used for the stars.

3.4 Model $\mathcal{FFC}$: Jupiter-mass objects as free-floating among the stars

For the models with free-floating jupiter-mass objects, model $\mathcal{FFC}$, we sprinkle the single planets from the primary-mass function (see model $\mathcal{SPP}$) in the cluster potential as single objects using the same initial distribution function as we used for the single stars. These models were run with 600 jupiter-mass objects (rather than 300 pairs in the other models).

We performed additional runs with 10^4 free floaters. Some of these runs have a different lower-limit to the mass function, but we keep the number of objects with a mass > 0.8 $M_{\rm Jup}$ at 600 (assuming that objects of lower-mass objects are unobservable).

Each simulation is stopped at an age of 1 Myr, after which we study the population of free floating jupiter-mass objects and the population of JuMBOs. A few simulations were extended to 10 Myr, to study the long term surviveability of JuMBOs.

In summary; we performed the following model calculations:

- $\mathcal{SPP}$: As outer orbiting planets
- $\mathcal{SPM}$: As bound planet-moon pair orbiting a star
- $\mathcal{ISF}$: In situ formation of jumbos
- $\mathcal{FFC}$: Free floating single planets.

In figure 3.4 we illustrate the four models with a schematic diagram.

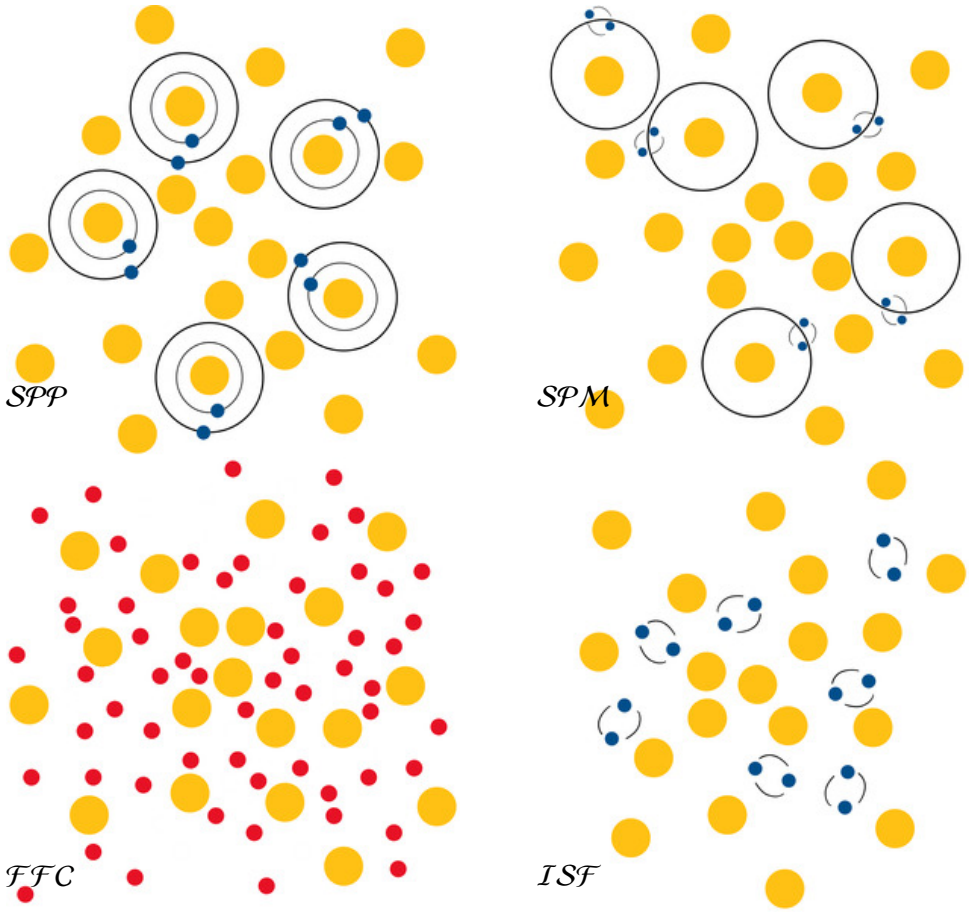

3.5 The simulations

All calculations are performed using 4-th order prediction-correction direct N-body integrator PH4 [36] through the Astrophysical MUltipurpose Software Environment, or AMUSE for short [37–39]. The data files are stored in AMUSE formatted particle sets, and available via zenodo `10.5281/zenodo.10149241`, and the source code is available at github `https://github.com/spzwart/JuMBOs`.

The script to run the simulations is fairly simple. It is essentially the same script from chapter 2 in [39], including the collision-detection stopping condition. Runs are performed with the default time-step parameter $\eta = 0.03$, which typically leads to a relative energy error $< 10^{-8}$ per step, and $< 10^{-5}$ at the end of the run. The fractal initial condiitons with small virial radius (0.25 pc) are, not surprisingly, the hardest runs to perform. The energy error in these runs can be somewhat higher at times, but never exceed $< 10^{-3}$, which according to [40], suffices for a statistically reliable result.

Snapshots were stored every 0.1 Myr, and the simulations were continued until 1.1 Myr. The data analysis is performed on the snapshots of the 1 Myr old cluster.

Although incorporating stellar evolution, general relativity and the Galactic tidal field would have been straightforward, we decided to ignore those. We do not expect any stars to effectively lose any mass during the short duration of the simulations, or the tidal field to have any influence on the close encounters in the simulations. Incorporating genera relativity would have made the calculations expensive without much astrophysical gain.

3.6 Finding JuMBOs

JuMBOs are soft in terms of the average local kinetic energy of the surrounding objects (stars and planets), and this makes them somewhat hard to find in the numerical models. One generally consider hard binary paris or multiples in direct N-body simulations are finding those soft pairs requires some extra effort. We search for JuMBOs by first selecting any object in the cluster, star or planet, and find the bound neares neighbors. Of one of these companions has another object as nearests neighbor, we adopt that as the close pair, and the initially selected object as the tertiary. Later, we order the particles in terms of distance and mass, on which the eventual designation is based. We recognice single stars s, and planets p (although we are uncertain weather or not to call these objects planets). Pairs of objects are then placed in parenthesis, for binary stars we write (s, s), a planetary system can be (s, p) (single planet) or $((s, p), p)$ (planet pair as in the $\mathcal{SPP}$ model) or $(s, (p, p))$ (planet pair orbiting a star as in the $\mathcal{SPM}$ model). JuMBOs in this terminology are indicated as (p, p).

4 Results

The main results of the calculations are presented in the tables table 1 and table 2.

In table 1 we list per model the different model outcomes. The various simulations results are named after their model designation followed by either the letter "Pl" for the Plummer model, or "Fr" for the Fractal model. The model name ends with the virial radius "R" in parsec, here 025 indicates 0.25 pc, 050 for 0.5 pc and 100 for 1 pc virial radius.

The $\mathcal{SPP}$ and $\mathcal{FFC}$ models systematically fail to reproduce the observed population of JuMBOs by a factor of 50 to 400. Changing the initial distribution in semi-major axis of the inner orbit from a uniform distribution to a logarithmic distribution reduces the formation rate of JuMBOs even further. There are some systematic trends in terms of cluster density and Plummer versus fractal distribution, but it is not clear how these models can lead to JuMBOs. Both models produce a considearble population of binary stars and single planetary systems, in particular in the fractal distributions, where the typical fraction of dynamically formed binary stars is around 4 %, and the fraction of plantary sytems 0.7 % per star.

Interestingly, the model that already start with some paired configuration with a star tend to produce more binaries and planetary systems, that the models where planet-mass objects do not orbit stars.

The high abunance of hierarchical multiple planets $(((s, p), p))$ in the $\mathcal{SPP}$_Pl and $\mathcal{SPM}$_Pl models reflects some of the initial conditions. These models also end to produce a relatively rich population of single planet systems (s, p).

The only models that produce a considerably population of JuMBOs are the $\mathcal{SPM}$ models and the $\mathcal{ISF}$. Where for the latter the Plummer distributions tend to produce sufficient number of JuMBOs whereas the fractal model produce too few.

To further mediate the discussion, we calculate orbital parameters for the surviving JuMBOs in the various models.

The median, the 25% and 75% quartiles for the JuMBO $((p, p))$ distribution for primary mass, secondary mass, semi-major axis and eccentricity are presented in table 2. The models that preduce too few JuMBOs to calculate the median and quartiles are omitted.

The primary masses produced in our models $\mathcal{SPM}$ and $\mathcal{ISF}$, tend to be a bit on the high side, but the secondary masses are in the observed mass range. The $\mathcal{SPM}$ models all tend to lead to orbits that are too tight. Leave out the $a < 25$ au JuMBOs does not improve the median orbital separation.

In terms of the orbital separation (or projected distance) the best model seems to be the $\mathcal{ISF}$ Plummer model with a 0.5 pc virial radius, but the distributions are wide, and the 1 pc $\mathcal{ISF}$ fractal

Table 1: The average number of systems per simulations model categorized in groups. The possible outcomes are the number of single stars (n_s), binaries ($n_{(s,s)}$), star orbited by a single planet ($n_{(s,p)}$), star orbted by two planets ($n_{((s,p),p))}$), single isolated planets (n_p) and JuMBOs($n_{(p,p)}$). Note that we only list those objects with a mass > 0.8 $M_{\rm Jup}$. As a consequence, the total number of planary mass objects does not always add up to 600. The number of stars also does not always adds up to 2500 because of collisions and hierarchies not listed in the table.

model	n_s	$n_{(s,s)}$	$n_{(s,p)}$	$n_{((s,p),p))}$	n_p	$n_{(p,p)}$
$\mathcal{SPP}$_Pl_R025	2287	0	84	129	258	0
$\mathcal{SPP}$_Pl_R050	2224	1	42	232	93	0
$\mathcal{SPP}$_Pl_R100	2204	0	19	277	26	0
$\mathcal{SPP}$_Fr_R025	2308	72	8	0	591	0
$\mathcal{SPP}$_Fr_R050	2279	83	28	6	560	0
$\mathcal{SPP}$_Fr_R100	2327	64	27	10	553	0
$\mathcal{SPM}$_Pl_R025	2480	0	17	3	413	18
$\mathcal{SPM}$_Pl_R050	2457	0	36	7	341	44
$\mathcal{SPM}$_Pl_R100	2464	0	22	14	394	15
$\mathcal{SPM}$_Fr_R025	2320	76	1	0	448	5
$\mathcal{SPM}$_Fr_R050	2293	90	2	0	444	17
$\mathcal{SPM}$_Fr_R100	2361	61	3	0	447	26
$\mathcal{ISF}$_Pl_R025	2498	0	0	0	425	23
$\mathcal{ISF}$_Pl_R050	2498	1	0	0	362	48
$\mathcal{ISF}$_Pl_R100	2500	0	0	0	246	108
$\mathcal{ISF}$_Fr_R025	2310	65	7	0	392	0
$\mathcal{ISF}$_Fr_R050	2309	81	7	0	450	4
$\mathcal{ISF}$_Fr_R100	2345	73	0	1	454	6
$\mathcal{FFC}$_Pl_R025	2271	87	11	0	580	0
$\mathcal{FFC}$_Pl_R050	2313	83	3	0	595	0
$\mathcal{FFC}$_Pl_R100	2331	75	5	0	593	0
$\mathcal{FFC}$_Fr_R025	2280	93	11	0	584	0
$\mathcal{FFC}$_Fr_R050	2308	75	12	0	1291	0
$\mathcal{FFC}$_Fr_R100	2314	83	3	0	805	1

Table 2: Simulation results for the models that produce a sufficiently large population of JuMBOs to be considered feasable (mainly models $\mathcal{SPM}$ and $\mathcal{ISF}$). We present the mean values and the quartile intervales for 25 % and 75 %.

model	$\langle M\rangle/M_{\rm Jup}$	$\langle m\rangle/M_{\rm Jup}$	$\langle a\rangle$/au	$\langle e\rangle$
$\mathcal{SPM}$_Pl_R025	$3.62^{+1.36}_{-2.68}$	$1.12^{+0.24}_{-2.14}$	$99.08^{+37.24}_{-36.38}$	$0.47^{+0.18}_{-0.13}$
$\mathcal{SPM}$_Pl_R050	$4.02^{+2.10}_{-3.71}$	$1.74^{+0.73}_{-0.93}$	$94.28^{+32.78}_{-78.90}$	$0.33^{+0.19}_{-0.27}$
$\mathcal{SPM}$_Pl_R100	$6.93^{+4.38}_{-3.07}$	$1.29^{+0.23}_{-1.22}$	$140.96^{+37.10}_{-11.20}$	$0.12^{+0.05}_{-0.27}$
$\mathcal{SPM}$_Fr_R025	$2.66^{+1.78}_{-3.20}$	$1.87^{+1.05}_{-0.37}$	$35.56^{+20.57}_{-62.84}$	$0.80^{+0.10}_{-0.18}$
$\mathcal{SPM}$_Fr_R050	$9.64^{+7.02}_{-1.99}$	$2.00^{+0.69}_{-0.58}$	$82.76^{+21.74}_{-83.04}$	$0.56^{+0.29}_{-0.18}$
$\mathcal{SPM}$_Fr_R100	$4.60^{+2.57}_{-2.44}$	$1.80^{+0.64}_{-2.47}$	$73.20^{+27.21}_{-100.43}$	$0.38^{+0.21}_{-0.13}$
$\mathcal{ISF}$_Pr_R025	$8.12^{+3.44}_{-4.51}$	$2.10^{+0.98}_{-1.66}$	$112.06^{+40.76}_{-181.76}$	$0.43^{+0.08}_{-0.19}$
$\mathcal{ISF}$_Pl_R050	$7.00^{+3.28}_{-4.23}$	$2.03^{+0.68}_{-0.99}$	$296.40^{+168.53}_{-190.04}$	$0.62^{+0.19}_{-0.12}$
$\mathcal{ISF}$_Pl_R100	$5.25^{+2.37}_{-3.16}$	$1.60^{+0.72}_{-1.40}$	$457.63^{+265.29}_{-193.56}$	$0.67^{+0.23}_{-0.14}$
$\mathcal{ISF}$_Fr_R025				
$\mathcal{ISF}$_Fr_R050	$4.82^{+3.05}_{-4.42}$	$1.38^{+0.75}_{-2.42}$	$37.57^{+15.07}_{-42.46}$	$0.77^{+0.06}_{-0.05}$
$\mathcal{ISF}$_Fr_R100	$10.15^{+3.75}_{-2.84}$	$1.98^{+0.50}_{-2.13}$	$97.05^{+47.34}_{-189.07}$	$0.77^{+0.17}_{-0.16}$
$\mathcal{FFC}$_Fr_R100	$6.57^{+0.00}_{-0.00}$	$2.47^{+0.00}_{-0.00}$	$846.35^{+0.00}_{-0.00}$	$0.98^{+0.00}_{-0.00}$

model could also consistent. We tend to prefer the former, though, because also the number of JuMBOs is somewhat consistent with the observations, as well as the number of free floateers.

The eccentricity distribution in the $\mathcal{SPM}$ Plummer models is systematically smaller than than in the fractal models. In these models, the planet-moon pairs started in almost circular orbits, whereas in the $\mathcal{SPM}$ they started with higher average eccentricities. In the fractal models, the eccentricities are more effectively perturbed and thermaized, whereas in the plummer models this did seem to have happened.

4.1 stellar and planetary collisions

In all our simulations, we never encountered a collision between two Jupiter-mass objects, but collisions with at least one star are not uncommon. Plummer models tend to have fewer (or no) collisions. the only Plummer models in which collisions among stars were common is in model $\mathcal{FFC}$ with 64, 20 and 18 collisions for those models with a viral radius of 0.25 pc, 0.5 pc and 1.0 pc, respectively. On average, 17% of the collisions occurs between a star and a planet-mass objects. Interestingly enough, the fractal models from the same series only experience 30, 17 and 14 collisions for the same virial radii.

In general, the fractal models all tend to experience collisions, but mostly among stars. The collision frequency drops roughly linearly with virial radius.

In general we argue that collision in Plummer models are rare (except in the presence of a large population of free floating planet-mass objects), that for the fractal models 83% of the collisions is between two stars and the rest between one star and one planet, and the collision frequency is inversely proportional with initial virial radius.

5 Discussion

We explore the possible origin of the rich population of jupiter-mass binary objects (JuMBOs) in the direction of the Trapezium cluster. The main problems in explaining the observations hides in the large number of jupiter-mass objects, their large binary fraction and the rather wide separations.

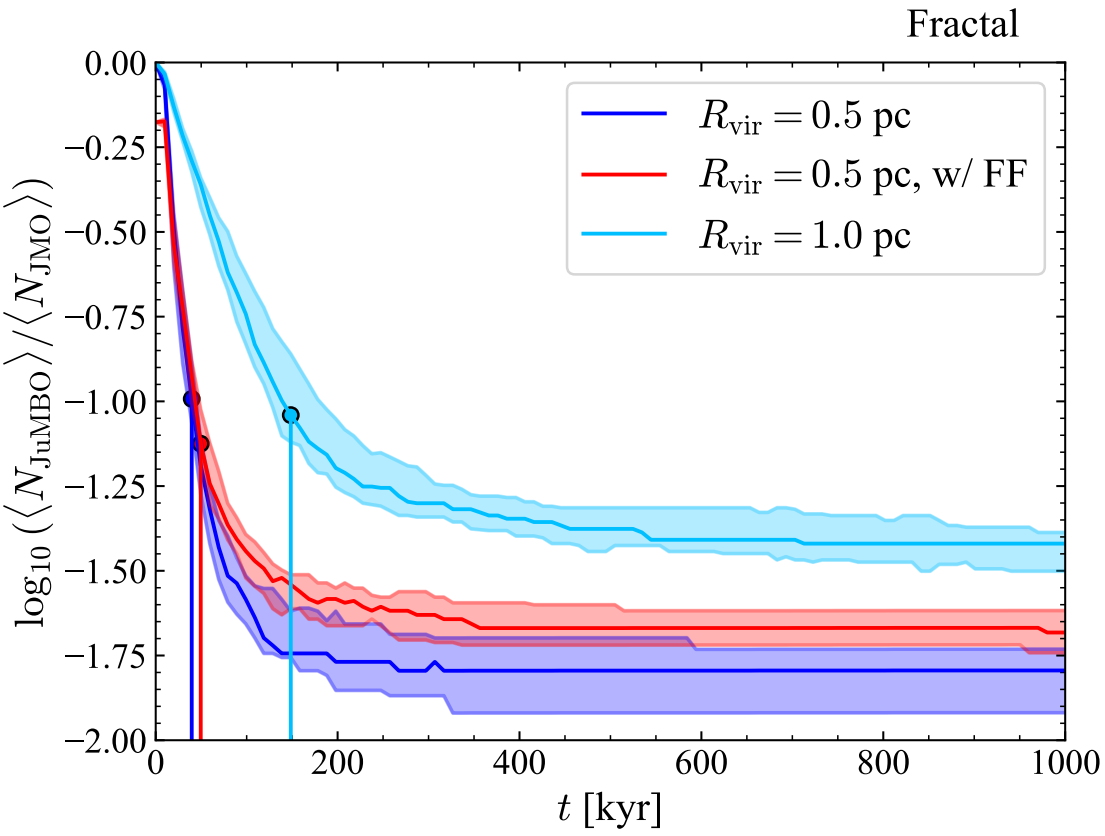

Figure 1: Fraction of jumbos as a function of time for models $\mathcal{ISF}$_Fr_R050 and $\mathcal{ISF}$_Fr_R100. The former model we also calculate with a population of single jupiter-mass objects. The number of free floating objects is the same as the number if primordial JuMBOs and their masses are taken from the primary mass function.

Assuming that they are bound, their orbits would be soft for any encounter in the cluster, and they are not expected to survive for more than a few kyr.

In figure 1 we illustrate how the fraction of jumbos decreases with time in models $\mathcal{ISF}$_Fr_R050 and $\mathcal{ISF}$_Fr_R100. The drop in the binary fraction among jupite-mass objects initially drop exponentially, to slow down after about 0.1 Myr at a survival fraction of $\sim 2\,\%$ for the 0.5 pc virial radius and $\sim 10\,\%$ for the 1 pc virial radius cluster. For the latter model, the fraction of JuMBOs drops eventually to about 4 %. Both fractions are lower than the observed 8 %. Starting with a tighter population of JuMBOs will help delaying their ionization, but at the cost of losing consistency with the distribution in the separation.

An alternative explanation for the large population of pairs among the free-floating jupiter-mass objects might be that they form late as binaries. If, for example, they only formed in the last ~ 0.3 Myr, their masses would have been understaimated, based on the cooling curves used in [1]. with the higher masses, the binaries would be somewhat harder, and therefore more difficult to ionize. This would delay their destruction, and the high binary fraction among the Jupiter-mass objects would stem from the surviving population.

The binary fraction continues to drop, and by the time the cluster is as old as Upper Scorpio (~ 10 Myr), very few JuMBOs would be left. Although, [5], reported the detection of 70 to 170 jupiter-mass objects none of them would be paired. With a 2% fraction of JuMBOs at an age of 10 Myr, we would naively expect Upper Scorpio to contain between 1 and 3 JuMBOs, where none were observed. Our calculations, on the other hand, did not include primordial binaries (or higher

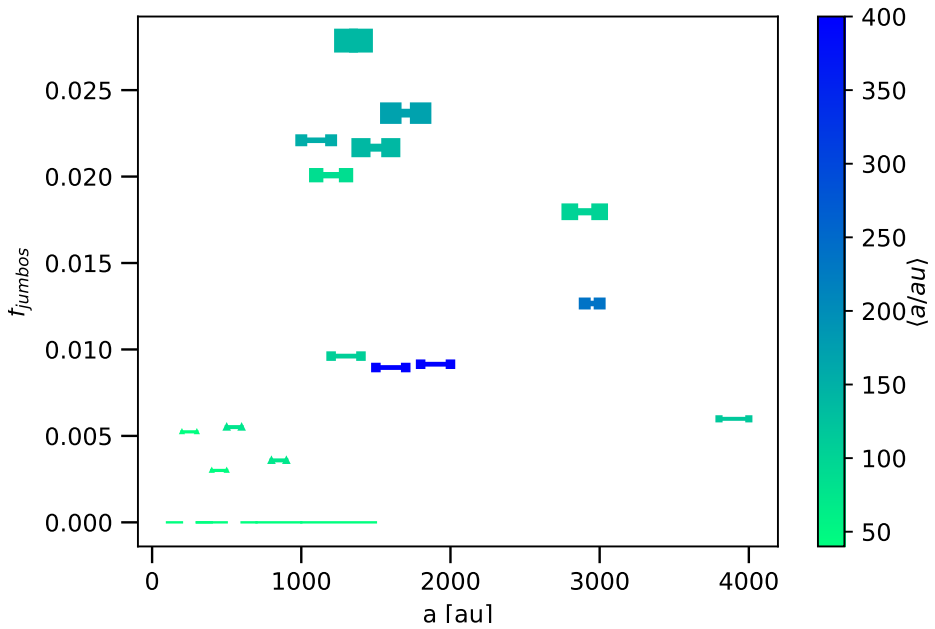

Figure 2: The number of jumbo's produced in model $\mathcal{SPP}$, as fraction of the number of free floating planets for various simulations starting with a Plummer sphere with a virial radius of 0.5 pc. The bullet points along each line correspond with the adopted orbital separation of the two planets (a_1 and a_2). The red symbols indicate an average orbital separations for the jumbos between 25 au and 380 au. The black symbols are outside this regime. The symbol sizes give the number of jumbos (see top right for scaling) in the particular simulation.

order systems, not did we take the effect of stellar evolution and supernovae into account. Those processes may have a profound effect of the fraction of JuMBOs, tending to reduce them rather then increase their number.

5.1 Failure of the $\mathcal{SPP}$ model

The $\mathcal{SPP}$ model systematically fail to reproduce the observed population of JuMBOs by a factor of 50 to 400. Changing the initial distribution in semi-major axis of the inner orbit from a uniform distribution to a logarithmic distribution reduces the formation rate of JuMBOs even further.

To further explore the failure of model $\mathcal{SPP}$, we perform an additional series of simulations with pre-determined inner and outer orbital separations a_1 and a_2 using the Plummer distribution with virial radii of 0.25 pc, and 0.50 pc for the stars. According to [27], the eventual orbital separation of the JuMBO would be consistent with the difference in orbital separation between the two planets when orbiting the star. For this reason we perform an additional series of runs with a mutual separation $a_2 - a_1 = 100$ au and $a_2 - a_1 = 200$ au, expecting those to lead to consistent results in comparison with the observations, as was argued in [27]. The results of these simulations are presented in figure 2.

For these models the JuMBO-formation efficiency peaks for an orbital separation $a_1 \gtrsim 1000$ au, but steeply drops for smaller values of a_1. As proposd by [27], we adopt a difference in the initial orbital distance of about $a_2 - a_1 = 100$ au or 200 au (see figure 2), which would lead to JuMBO orbits in the same range. We performed a total of 45 calculations with various ranges of a_1 and a_2, of which 39 produced a total of 910 JuMBOs. The initial mean value of $a_1 - a_2 = 167 \pm 38$ au, leading to a final orbital separation of the jumbos of $a_j \sim 262 \pm 45$ au. The claim made by [27], that

the separation distance $a_2 - a_1$ leads to JuMBOs with a similar orbital distance seems reasonable.

The rate, derived by [27], however, appears to be orders of magnitude smaller than they expected. They calculate the rate by means of 4-body scattering experiments, in which a star with two equal-mass planets with semi-major axes a_1 for the inner and a_2 for the other planet, encounters a single star. Their largest cross section of roughly a_1^2 is obtained if the encounter velocity $0.8 v_\star / v_1$. For an encounter at the cluster's velocity dispersion, the inner planet would then have a orbital separation of about 900 au around a 1 $M_\odot$ star.

5.2 The failure of model $\mathcal{SPP}$

Note that an inner orbital separation of $a_1 = 800$ au for a 10 $M_{\rm Jup}$ planet leads to a Hill radius of about 150 au. An orbit with $a_2 = 1000$ au, is probably only marginally stable. Still, even in those runs the total number of JuMBOs remains small compared to the number of free floaters.

In [27], the highest cross section is achieved for the orbital velocity of the inner-most planet as fraction of the typical encounter velocity $v1/v_{\rm disp} \sim 0.8$. With a cluster velocity dispersion of ~ 0.8 km/s, the orbital velocity roughly 1 km/s. Around an 1 $M_\odot$ star such a velocity is obtained, assuming a Kepler orbit, at an orbital separation of 800 au. It turns out, that the results of the cross section calculations performed by [27] are consistent with our direct N-body simulation, but that the adopted initial orbital separation is too wide in comparison with a realistically population of inner planetary orbits for jupiter-mass planets. Observational selection effect in finding $\gtrsim 800$ au jupiter-mass planets are quite severe, but we consider it unrealistic to have 600 out of 2500 stars to be orbited by such wide planetary systems. In particular, when one considers the small sizes of the observed disks in the Trapezium cluster, which today are all smaller than 400 au [41].

5.3 Further constraining the initial conditions for model $\mathcal{ISF}$

With the current models, we can further constrain the model parameters by repeating several calculations for better statistics and exploring other parts of the parameter space. We peroform this analysis for model $\mathcal{ISF}$, because that model seems to be most viable for producing a sufficiently large population of JuMBOs and reproduces the observed orbital characteristics. Using the results of the general models, we alter our initial conditions with the aim of mimicking observations. Doing so allows us to disentangle aspects of the cluster history, allowing for predictions on the properties of JuMBO formation. These runs correspond to the middle segment of table 4.

For all models, we constrain $n_{\rm JuMBO} + n_{\rm FF}$ to values reflecting the total planetary-mass population observed in [1], keeping in mind the survival rate of JuMBOsystems based on previous results to decide on the initial value of $N_{\rm JuMBO}$. The range of mass ratio and mass value remains unchanged. However, now the mass ratio follows a thermal distribution to reflect the abundance of $q = 1$ observations, whilst the mass of the objects follows a power-law distribution with $\alpha = -1.2$. The semi-major axis is uniformly distributed between the restricted range $a \in [25, 100]$ au. Here, the lower bound reflects the restrictions of observational resolution in the original study [1].

Models Fr_R050C and Fr0FFOC look at scenarios where the initial JuMBO population has an eccentricity ranging between $e \in [0, 0.2]$ sampled from a uniform distribution. For all other models, the eccentricity remains thermalised and ranges between $e \in [0, 0.9]$.

5.4 $\mathcal{FFC}$: Free Floating Jupiter Mass Objects

In our final scenario, $\mathcal{FFC}$, we scatter 10^4 Jupiter-mass objects in the cluster with no JuMBO systems initialised. The main aim is to see the efficiency of forming JuMBOs via mutual captures of free floaters. The parameters of the cluster and free floaters remain unchanged to those listed in section **??**.

Table 3: Initial conditions of the various configurations. The nomenclature is as follows: The first letter identifies the cluster distribution. The number denotes the initial virial radius, 'FF' denotes the presence of Jupiter-mass free floaters, 'x' whether the system contains an abundance (excessive/extra) amount of these free floaters, 'O' denotes systems whose JuMBOshave their initial parameters constrained by the observational data and finally 'C', systems whose initialised JuMBOs are on circular orbits. Column 1: The model used. Column 2: The number of simulations for the given configuration. Column 3: The initial virial radius of the system. Column 4: The number of initialised JuMBOs. Column 5: The number of initialised free floaters.

Model	$N_{\rm runs}$	$R_{\rm vir}$ [pc]	$N_{\rm JuMBO}$	$N_{\rm FF}$
F05	20	0.5	500	0
F05FF	20	0.5	500	500
F1	20	1.0	500	0
P05	20	0.5	500	0
P05FF	20	0.5	500	500
P1	20	1.0	500	0
F05O	10	0.5	275	0
F05FFO	10	0.5	170	400
F05OC	10	0.5	275	0
F05FFOC	10	0.5	170	400
P05FFO	10	0.5	60	500
F05FFxJ	5	0.5	500	10^4
F05FFx	5	0.5	0	10^4

Table 4: Initial conditions of the various configurations. The nomenclature is as follows: The first letter identifies the cluster distribution. The number denotes the initial virial radius, 'FF' denotes the presence of Jupiter-mass free floaters, 'x' whether the system contains an abundance (excessive/extra) amount of these free floaters, 'O' denotes systems whose JuMBOs have their initial parameters constrained by the observational data and finally 'C', systems whose initialised JuMBOs are on circular orbits. Col. 1: The model used. Col. 2: The number of simulations for the given configuration. Col. 3: The initial virial radius of the system. Col. 4: The number of initialised JuMBOs. Col. 5: The number of initialised free floaters.

Model	$N_{\rm runs}$	$R_{\rm vir}$ [pc]	$N_{\rm JuMBO}$	$N_{\rm FF}$
F05	20	0.5	500	0
F05FF	20	0.5	500	500
F1	20	1.0	500	0
F05FFL	5	0.5	500	500
P05	20	0.5	500	0
P05FF	20	0.5	500	500
P1	20	1.0	500	0
F05O	10	0.5	270	0
F05FFO	10	0.5	200	140
F05OC	10	0.5	270	0
P05FFO	10	0.5	70	400

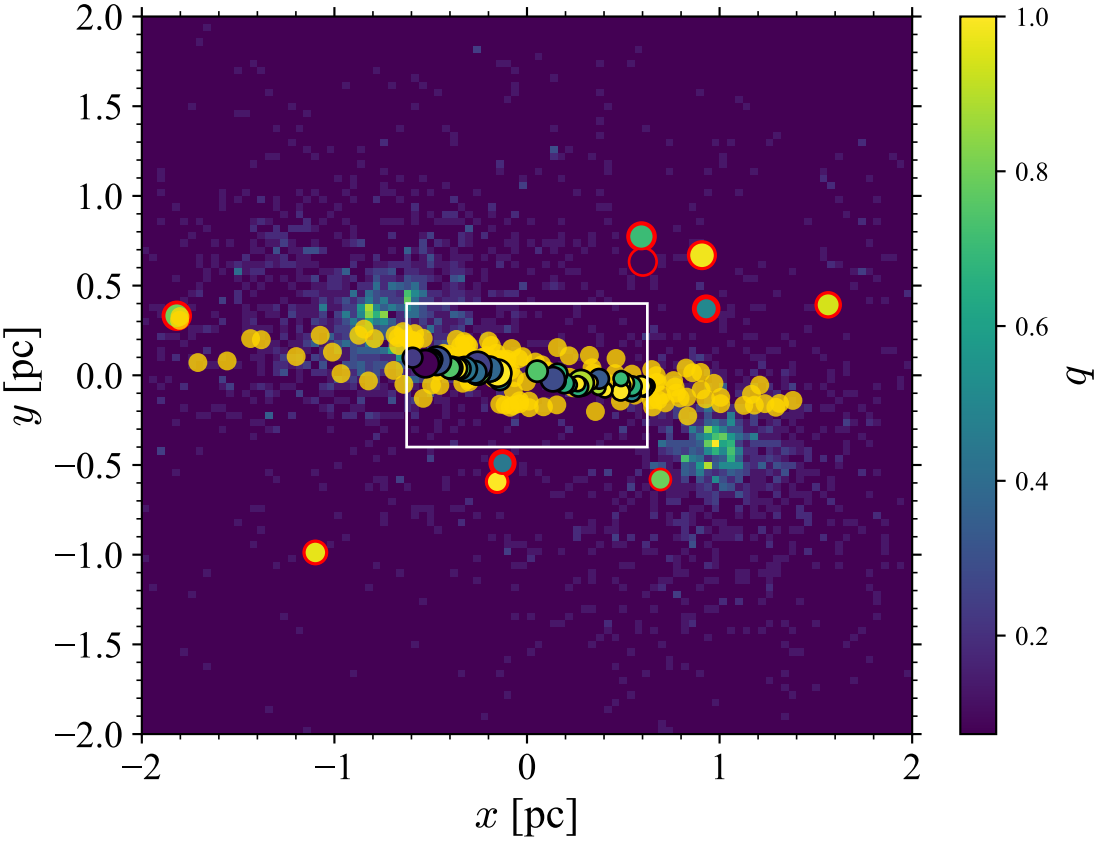

Figure 3: Schematic of a F05 simulation. The density map denotes final positions of simulated objects, the translucent yellow points observed stars taken from [**?**, **?**]. The white frame denotes the observed region in [1], with black outlined dots denoting observed JuMBOs. Red outlined dots denote the final JuMBOs observed in our simulation.

Table 5: Statistics on the surviving JuMBOs. ⟨...⟩ gives the median, while the ± denote where the lower and upper quartile lie. Col. 1: The fraction of JuMBOs present at the end of the simulation relative to the number initialised. Col. 2: The fraction of JuMBOs with projected separation, $r_{\rm ij} > 25$ au. Col. 3: The mass ratio of JuMBO systems. Col. 4: The primary mass of the JuMBO system. Col. 5: The semi-major axis of the JuMBO system. Col. 6: The eccentricity of the system.

Model	$f_{\rm surv}$	$f_{r_{ij}\geq 25{\rm au}}$	$\langle q\rangle$	$\langle M_{\rm prim}\rangle$ [$M_{\rm Jup}$]	$\langle M_{\rm sec}\rangle$ [$M_{\rm Jup}$]	r_{ij} [au]	$\langle a\rangle$ [au]	$\langle e\rangle$
F05	$0.02^{+0.00}_{-0.00}$	$0.67^{+0.19}_{-0.07}$	$0.61^{+0.21}_{-0.24}$	$8.6^{+2.4}_{-3.3}$	$4.2^{+3.2}_{-1.9}$	38^{+52}_{-18}	39^{+50}_{-16}	$0.67^{+0.16}_{-0.19}$
F05FF	$0.04^{+0.00}_{-0.01}$	$0.61^{+0.02}_{-0.11}$	$0.54^{+0.24}_{-0.24}$	$8.8^{+2.7}_{-2.6}$	$3.9^{+2.5}_{-2.0}$	30^{+43}_{-16}	37^{+41}_{-20}	$0.62^{+0.14}_{-0.21}$
F1	$0.04^{+0.00}_{-0.01}$	$0.72^{+0.11}_{-0.06}$	$0.60^{+0.20}_{-0.24}$	$8.3^{+2.4}_{-3.0}$	$3.8^{+2.4}_{-1.9}$	64^{+98}_{-40}	67^{+83}_{-38}	$0.68^{+0.16}_{-0.19}$
F05FFL	$0.03^{+0.00}_{-0.00}$	$0.46^{+0.07}_{-0.07}$	$0.57^{+0.31}_{-0.25}$	$8.1^{+2.9}_{-2.7}$	$2.7^{+3.1}_{-1.0}$	33^{+20}_{-18}	20^{+15}_{-9}	$0.61^{+0.20}_{-0.19}$
P05	$0.37^{+0.01}_{-0.02}$	$0.94^{+0.02}_{-0.01}$	$0.55^{+0.23}_{-0.23}$	$8.3^{+2.7}_{-3.1}$	$3.6^{+2.7}_{-1.8}$	233^{+234}_{-137}	268^{+237}_{-152}	$0.68^{+0.16}_{-0.22}$
P05FF	$0.52^{+0.02}_{-0.00}$	$0.92^{+0.00}_{-0.01}$	$0.57^{+0.21}_{-0.24}$	$8.1^{+2.8}_{-3.2}$	$3.4^{+2.7}_{-1.7}$	162^{+167}_{-94}	187^{+176}_{-106}	$0.61^{+0.14}_{-0.18}$
P1	$0.72^{+0.02}_{-0.01}$	$0.97^{+0.00}_{-0.01}$	$0.54^{+0.24}_{-0.23}$	$7.8^{+3.0}_{-3.0}$	$3.3^{+2.5}_{-1.6}$	344^{+271}_{-188}	396^{+250}_{-206}	$0.68^{+0.16}_{-0.20}$
F05O	$0.02^{+0.00}_{-0.01}$	$1.00^{+0.00}_{-0.16}$	$0.81^{+0.09}_{-0.17}$	$4.0^{+2.6}_{-1.9}$	$2.8^{+1.7}_{-1.5}$	61^{+46}_{-24}	67^{+48}_{-22}	$0.67^{+0.14}_{-0.19}$
F05FFO	$0.03^{+0.00}_{-0.00}$	$0.8^{+0.02}_{-0.15}$	$0.76^{+0.10}_{-0.17}$	$3.4^{+3.4}_{-1.7}$	$1.8^{+2.0}_{-0.8}$	44^{+37}_{-18}	46^{+38}_{-22}	$0.69^{+0.15}_{-0.18}$
F05OC	$0.02^{+0.01}_{-0.00}$	$0.67^{+0.19}_{-0.07}$	$0.81^{+0.10}_{-0.14}$	$4.7^{+3.2}_{-2.7}$	$3.6^{+2.6}_{-2.02}$	46^{+36}_{-26}	49^{+28}_{-28}	$0.45^{+0.33}_{-0.23}$
P05FFO	$0.76^{+0.01}_{-0.01}$	$0.89^{+0.03}_{-0.03}$	$0.78^{+0.12}_{-0.15}$	$3.7^{+3.5}_{-2.1}$	$2.1^{+2.5}_{-1.2}$	90^{+86}_{-44}	105^{+86}_{-47}	$0.61^{+0.15}_{-0.17}$

Figure 3 shows the final snapshot of a F05 simulation. It represents the typical final state of simulations evolved during our $\mathcal{ISF}$ and $\mathcal{FFC}$ runs. The density map reveals the final positions of all objects simulated. Surviving JuMBOs are scattered onto the plot with red outlines. Overlayed are also the positions of known stars (in yellow) taken from [**?**, **?**] and the positions of known JuMBOs (black outlined points) [1].

Table 5 summarises all our final results. We begin our discussion on the $\mathcal{ISF}$ models by looking at the general models (top segment of table 4).

Overall, JuMBOs are more likely to survive in a Plummer-like cluster. Their survival rates increase by a factor of $\sim$ 18 compared with likewise configurations initialised under a Fractal distribution. Even so, no configuration is successful in reproducing the 9% fraction of JuMBOs relative to free-floaters observed. Instead, in the $\mathcal{ISF}$ scenarios, the fraction of JuMBOs to JMO free floaters ranges between $0.29 \sim 1.3$ for Plummer runs and $0.01 \sim 0.02$ for Fractals.

The increase of JuMBO surviveability in runs including free-floaters could be due to the rare JMO-JuMBOinteraction hardening the binary, also resulting in a decrease in its gravitational cross section. We believe this to be the case even though as discussed in the introduction JuMBOs will tend to ionise, even when interacting with other JMO, since, although increasing the number of JMOs enhances the chances of two free-floaters (or a free floater and ionised JMO) settling into a newly formed binary, on average, only 0.4 new JuMBO systems emerge per run for F05 runs compared to the 0.65 in F05FF (from 1.75 to 3.15 between P05 and P05FF).

Figures 4 show the cumulative distribution function (CDF) for the semi-major axis of surviving JuMBOs during F05, F05FF and F1 runs. The Fractal distribution efficiently prunes off any wide orbits since its violent nature provokes many encounters result in the ionisation of JuMBO systems, moreso the ones on wide orbits who have a larger cross-section. The tendency for JuMBOs to ionise at any encounter is reflected by the little variation between runs of the same virial radius. We also note the tendency for JuMBOs to ionise even when a JMO perturbs the system as reflected with the decrease in median semi-major axis between models P05 and P05FF from $\langle a\rangle \sim 268$ au

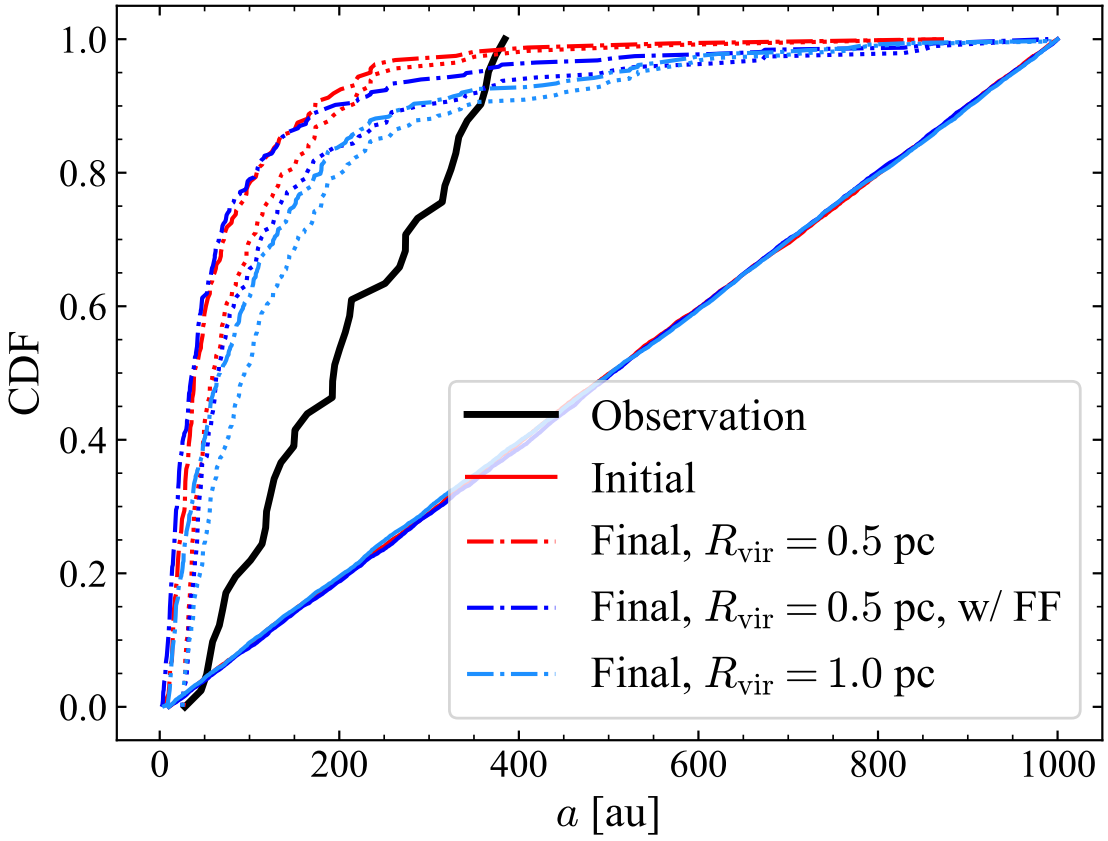

Figure 4: CDF of surviving JuMBO semi-major axis distribution for models F05, F05FF, F1. Dash-dotted curves incorporate all JuMBO systems, whereas dotted ones only those with a projected separation exceeding 25 au.

to $\langle a \rangle \sim 187$ au.

The results in semi-major axis' during the Fractal runs are much smaller than those observed, suggesting the $\mathcal{ISF}$ model fails to capture the birth of such environments. Contrariwise, and as seen in figure 5, Plummer models are capable of preserving the wider orbits. This, however, is due to the environment to output similar values to those inputted since it is less violent by nature.

Indeed, keeping in mind that our JuMBOs in these models are initialised with a uniform mass distribution, we see the uniformity reflected in the final $M_{\rm prim}$ vs. q parameter space shown in figure 6. Although it also fails at reproducing observations, figure 7 shows more structure and less uniformity in the distribution of JuMBOs in ($M_{\rm prim}$, q)-space as reflected by the starker contrasts between contour levels and smaller high-density regions.

Given this, although a correct calibration of initial conditions during Plummer runs will give back JuMBOs with similar properties to those observed, the extent of fine tuning needed and lack of natural mechanism to remove the tail end of wide-orbit JuMBOs, we can apply Occam's razor to rule it out as an initial conditions.

The omission of Plummer models is further supported since no systems formed dynamically during the runs. This contradicts with the observed presence of two triple JMO systems. Given this, we restrict ourselves to Fractal models as we believe this better represents the Trapezium cluster, a fact agreeing with [31].

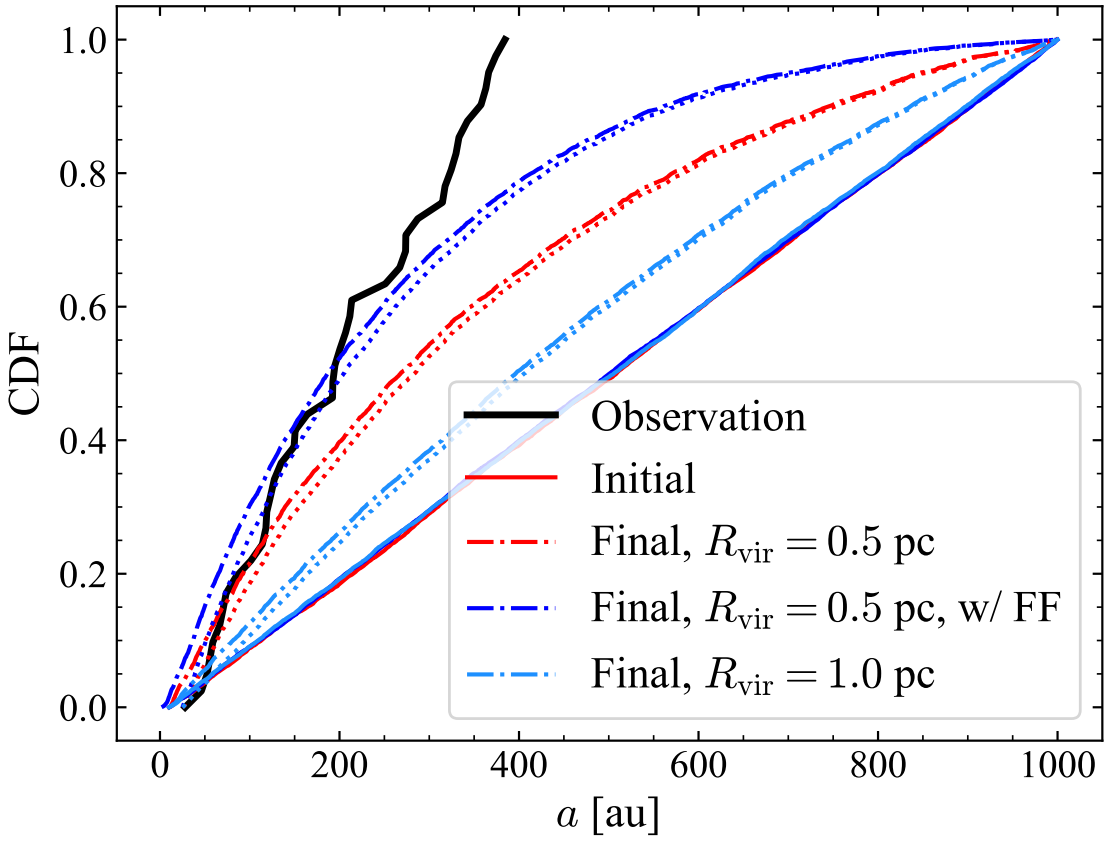

Figure 5: CDF of surviving JuMBO semi-major axis distribution for models P05, P05FF, P1. Dash-dotted curves incorporate all JuMBO systems, whereas dotted ones only those with a projected separation exceeding 25 au.

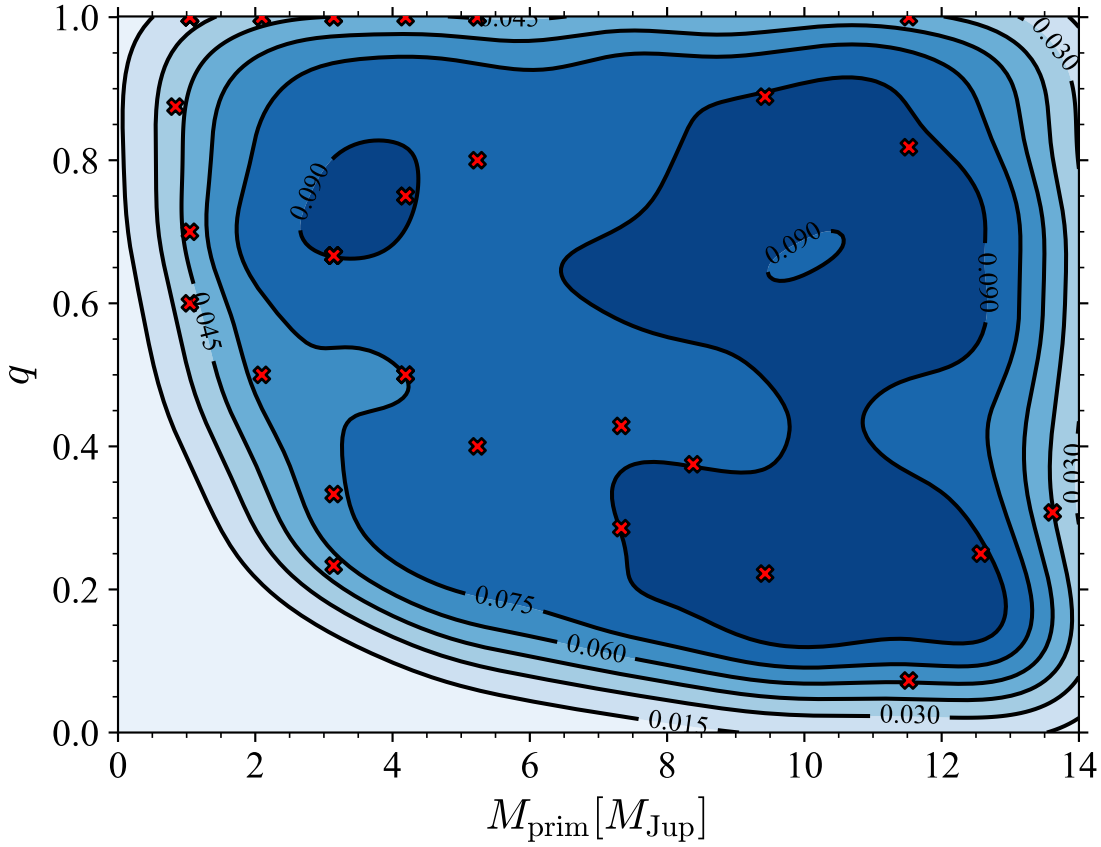

Figure 6: Contour plot of M_{prim} vs. q for model P05FF. Red crosses denote where observed JuMBOs lie.

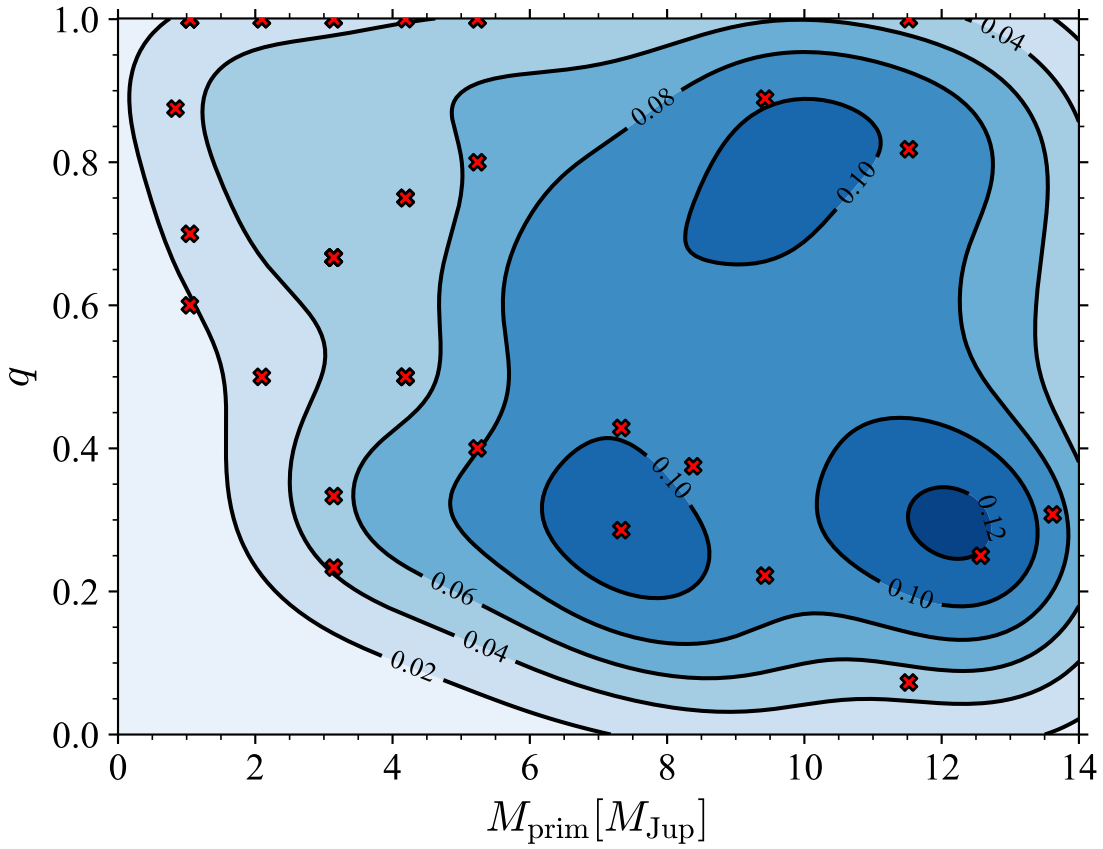

Figure 7: Contour plot of $M_{\rm prim}$ vs. q for model F05FF. Red crosses denote where observed JuMBOs lie.

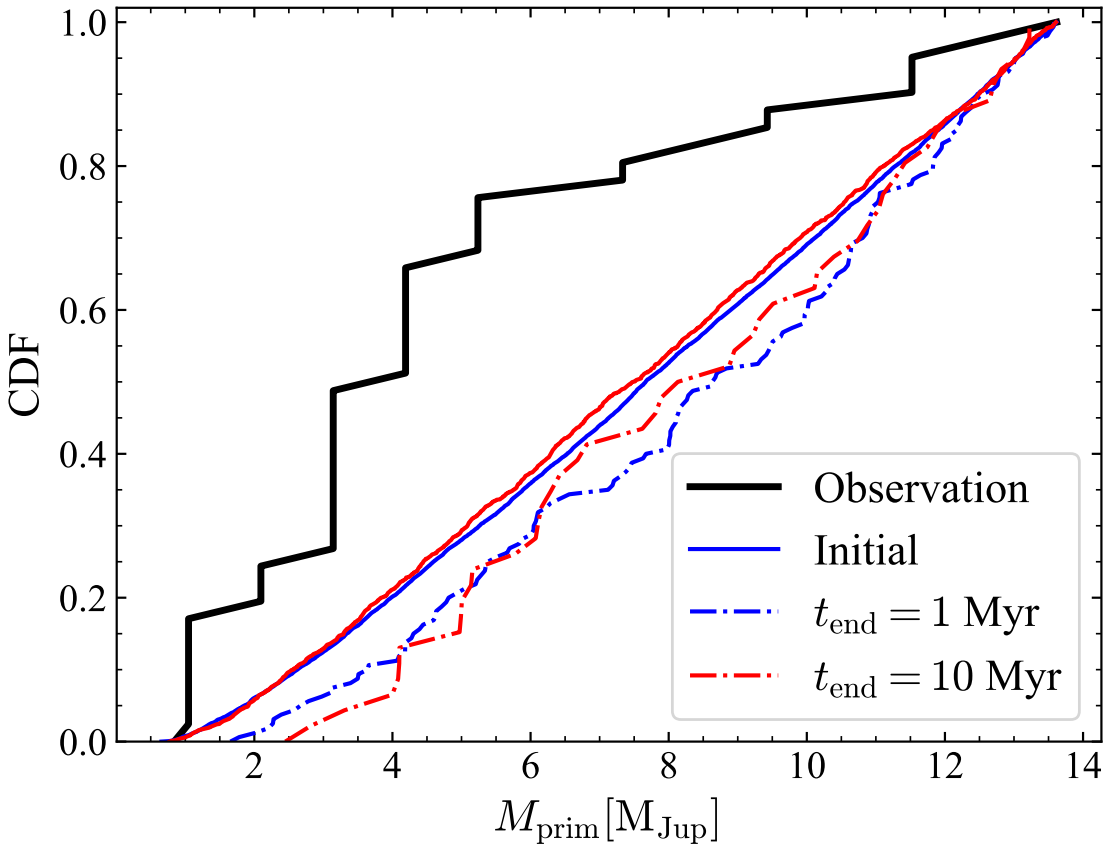

Figure 8: CDF of surviving JuMBO $M_{\rm prim}$ for models F05FF and F05FFL.

5.4.1 Evolving till 10 Myr

Here we analyse results for a system evolved to 10 Myr, with the aim of looking at the survival of JuMBOs in more established systems. Overall, the JuMBO survival rate decreases and the ones surviving exhibit tighter orbits with $\langle a \rangle \sim 20$, a regime in which two 3 $M_{\rm Jup}$ systems become hard for $\sim M_{\rm Jup}$ interactions.

Figure 8 shows the distribution of $M_{\rm prim}$ of surviving JuMBOs. The little difference observed between F05FF and F05FFL is reflected by the similarities between their median and interquartile (IQR) range ($\langle M_{\rm prim} \rangle \sim 8.8$ and $\langle M_{\rm prim} \rangle \sim 8.1$ for F05FF and F05FFL respectively). The fact that this holds for all configurations simulated implies the ease at which JuMBO systems ionise upon interaction.

Figure 9 shows the contour plot of $M_{\rm prim}$ vs. q. As before, the parameter space poorly replicates the observed distribution with most of the JuMBOs having too large a primary mass. We keep this in mind for simulations in the following subsection where we initialise JuMBOs with a power-law of $\alpha = -1.2$, the power-law found to best fit observations.

5.4.2 Observational Constraints

Our preliminary exploration allows us to rule out Plummer models and further constrain the parameter space. When applying these more restricted initial conditions, $f_{\rm surv}$ and e barely changes while a shows only marginal changes.

This slight increase in $f_{r_{ij} \geq 25\ {\rm au}}$, $\langle a \rangle$ and $\langle r_{ij} \rangle$ could be attributed to the reduction of JMO and JuMBOs present in the environment and the smaller masses they occupy making it harder for them

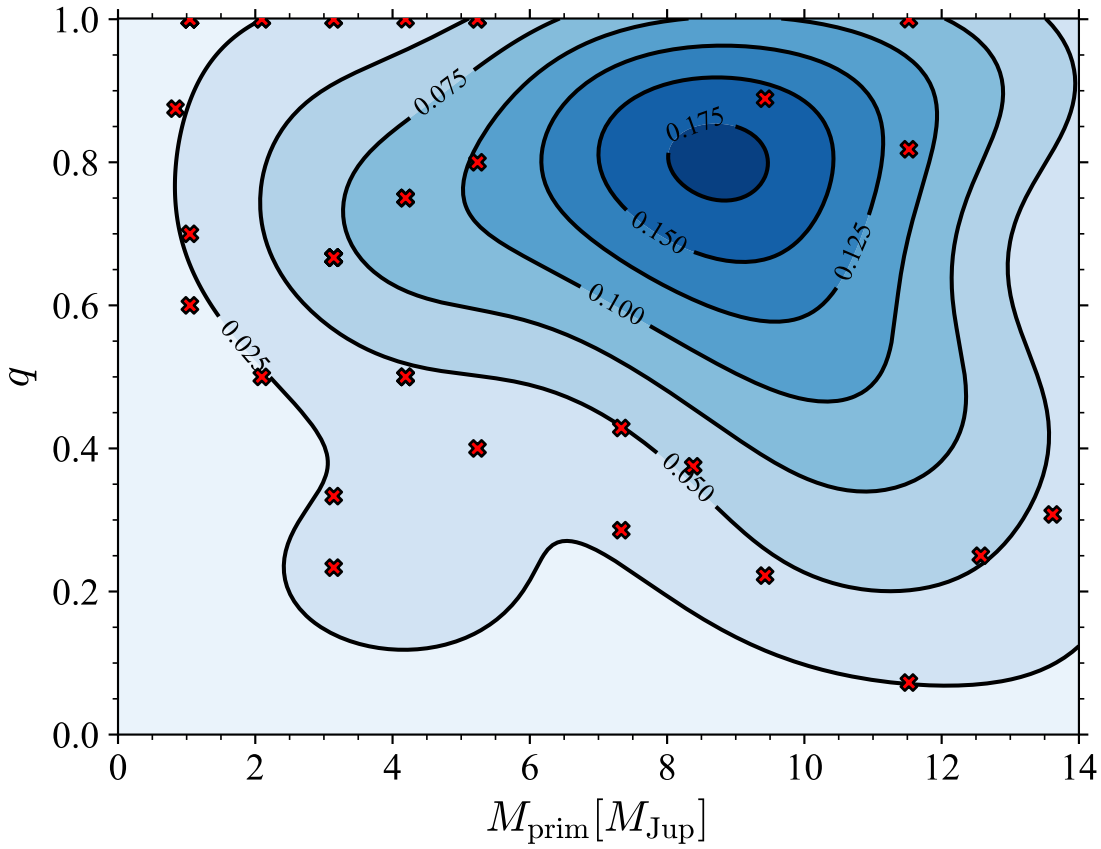

Figure 9: $M_{\rm prim}$ vs. q contour plot for model F05FFL. Red crosses denote where observed JuMBOs lie.

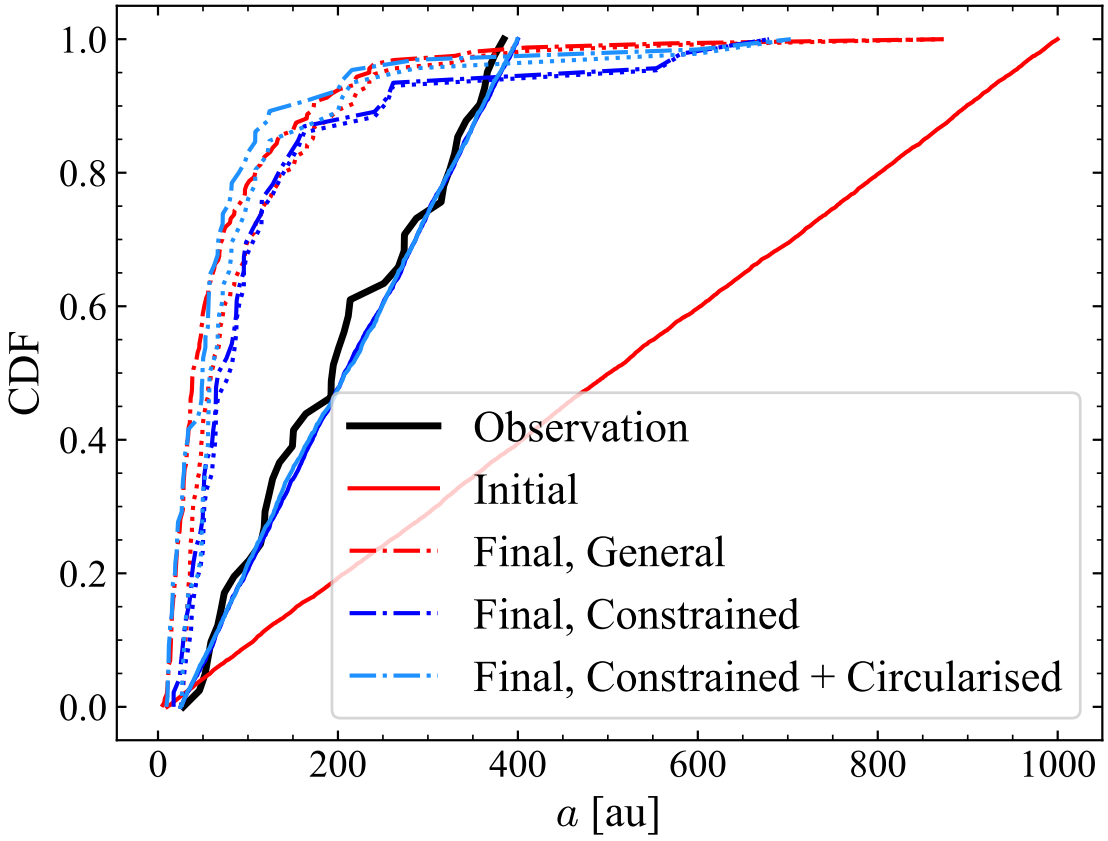

Figure 10: CDF of surviving JuMBO semi-major axis distribution for models F05, F05O, F05OC.

to destabilise wide binaries. The difference in the semi-major axis distribution between models F05, F05O and F05OC (JuMBOsare initially on circular orbits) is shown in figure 10. No matter the configuration, the Fractal models exhibit a natural tendency for trimming out wide binaries.

Figure 11 shows the CDF of primary masses comparing models F05, F05O And F05OC. No matter the configuration, a similar evolution is observed where surviving JuMBOs tend to have larger primary masses. However, unlike the F05 model, the constrained model, initialised with $\alpha = -1.25$, end up being roughly uniform in primary mass compared to the somewhat thermal appearance for F05. In doing, the median primary masses shift towards lower values while the mass ratio towards larger one. A fact reflected by the statistics shown in table 5 and shown in figure 12.

Over the course of our simulation, Fractal runs exhibit a range of dynamical phenomena. The statistics of merging scenarios, and the emergence of both Jupier-mass - Stellar binary systems and $N \geq 3$ systems are summarised in table 6.

Jupiter-mass - stellar mergers could ..... In addition to mergers, ejection events also occured. Though no JuMBOs were ejected, $\sim$ 1 JMO was ejected per simulation and $\sim$ 3 stellar-mass objects.

Figure 13 shows where in (a, e)-space Jupiter-mass - Stellar binaries lie, with little variation between configurations. The parameter space is widely covered, with signs of low-eccentricity but very wide ($a \geq 700$ au) binaries. Nevertheless, the vast majority exhibit large eccentricities and semi-major axis, reflecting their dynamical origin. The non-negligible amount of these systems emerging provide an interesting prospect of detecting ultra-cold Jupiters orbiting stars who have recently fostered them.

Given the poor reproducability in ratios of JuMBOs to JMO free floaters and the tight orbits

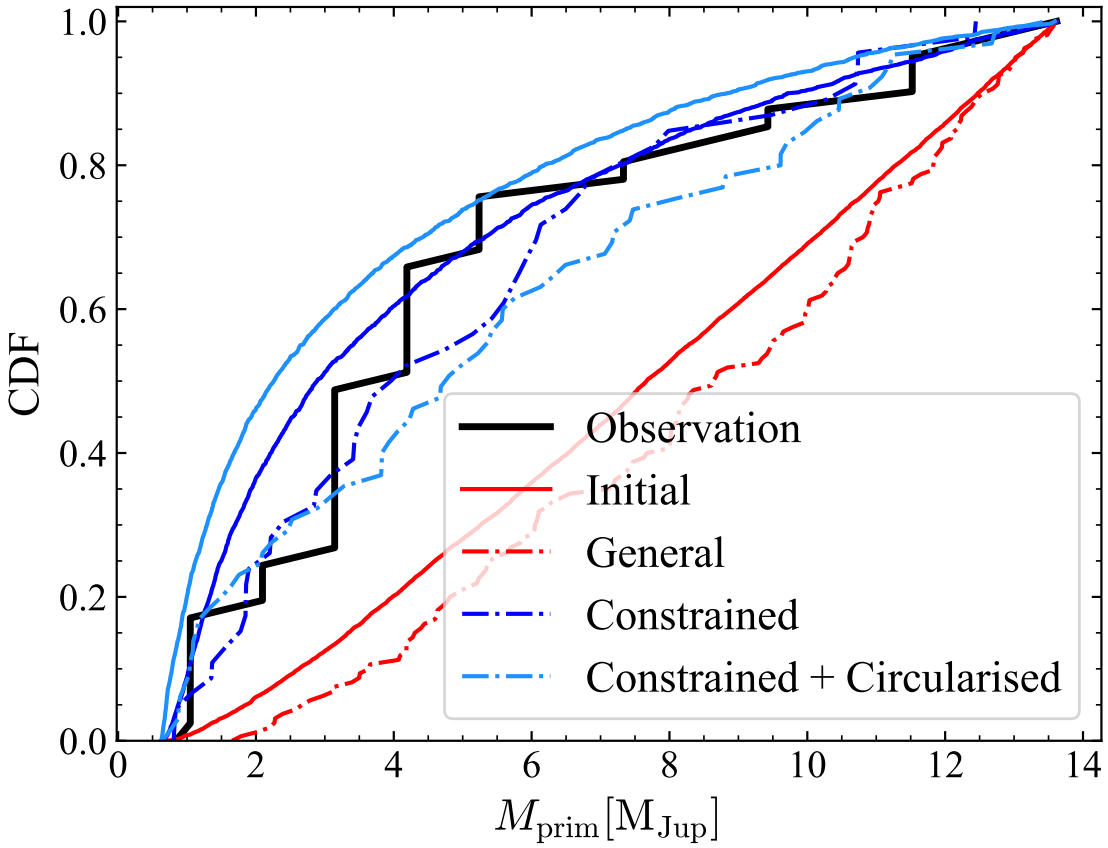

Figure 11: CDF of surviving JuMBO primary mass for models F05, F05O, F05OC.

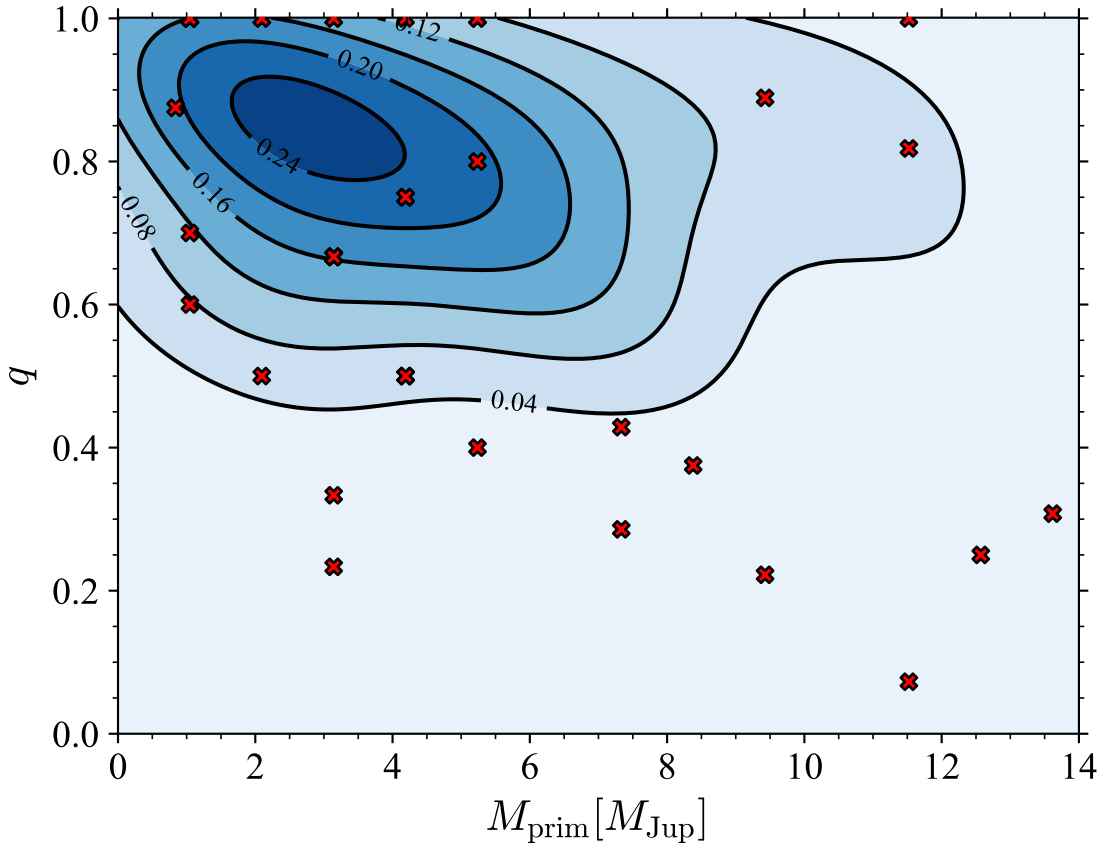

Figure 12: Contour plot of $M_{\rm prim}$ vs. q for F05O. Red crosses denote where observed JuMBOs lie.

of JuMBOs we conclude that the $\mathcal{ISF}$ models are most likely not the origins of JuMBOs, lending us to our final possible scenario, $\mathcal{FFC}$.

5.5 $\mathcal{FFC}$

6 Conclusions

The discovery of relatively wide pairs of jupiter-mass planetary objects in the Trapezium cluster emphasizes our limited understanding of low-mass star and planet formation. In order to derive characteristcs for their origin we performed simulations of Trapezium-equivalent stellar clusters (2500 stars with a virialized ~ 0.5 pc radius) with various compositions of planetary objects and stars.

Models in which planets form in wide circum-stellar orbits, as proposed by [27], produce many single free floating planets, but an insufficient number of planet pairs per cluster. The ratio of single to pairs of planets is too low by a factor of 60 to 400.

The models in which pairs of planetary-mass objects orbit stars in the form of a planet-moon system, produce many free floating planetary pairs, and in the proper range of orbits. In particular the models that start with fractal initial conditions tend to produce a fraction of jumbos of among free floating planets $O(0.1)$, which is close to the observed value of 0.078 ± 0.012. The absolute numbers are a bit high though, by a factor of two, but that is easily solved by starting with fewer systems. Although the distribution in orbital separation matches the observations by constructing the initial conditions appropriately, these models prediction rather low-eccentricities ($e \lesssim 0.4$).

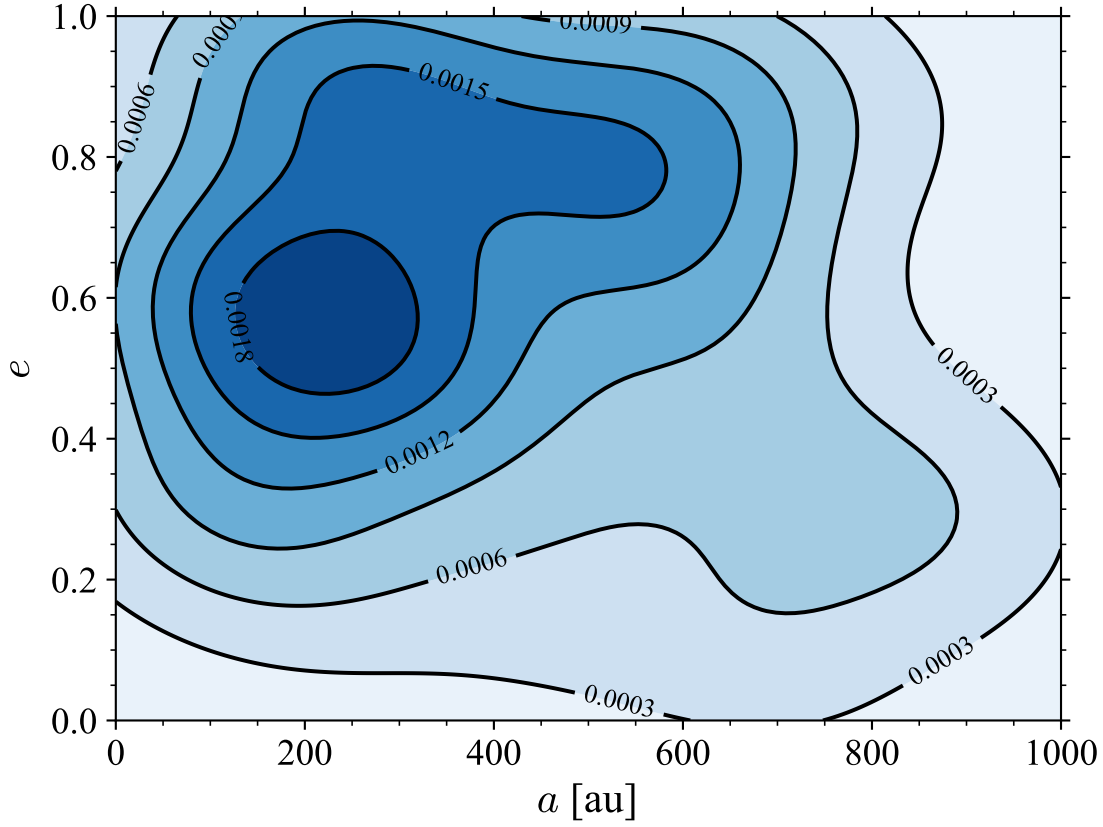

Figure 13: a vs. e parameter space occupied by Star-JMO binaries during F05FFO runs.

Table 6: TO CHECK

Model	$\langle N_{\rm JS,merge} \rangle$	$\langle N_{\rm SS,merge} \rangle$	$\langle N_{\rm JS} \rangle$	$\langle N_{\rm multi} \rangle$
F05	$2.5^{+0.5}_{-1.5}$	19^{+4}_{-7}	8^{+3}_{-0}	2^{+0}_{-0}
F05FF	$5.5^{+1.5}_{-1.5}$	21^{+2}_{-4}	14^{+1}_{-3}	2^{+0}_{-0}
F1	$1.0^{+1.0}_{-0.0}$	14^{+3}_{-5}	10^{+1}_{-3}	2^{+0}_{-0}
F05FFL	$5.0^{+0.0}_{-1.0}$	22^{+3}_{-5}	$1.0^{+0.0}_{-0.0}$	0^{+7}_{-0}
F05O	$2.0^{+0.8}_{-1.8}$	25^{+2}_{-8}	$4.5^{+2.8}_{-0.5}$	2.0^{+0}_{-0}
F05FFO	$1.0^{+1.0}_{-0.0}$	17^{+3}_{-1}	$5.0^{+1.5}_{-1.0}$	1.0^{+0}_{-0}
F05OC	$0.5^{+2.3}_{-0.5}$	20^{+5}_{-4}	$4.5^{+1.5}_{-1.5}$	3.5^{+0}_{-0}

For the model to produce a sufficient number of JuMBOs it requires planet-moon pairs form in $\gtrsim 1000$ au orbits around their parent star. Such wide orbits are exotic considering the fact that the circum-stellar disks observed in the Trapezium cluster tend to be smaller than 400 au. We therefore do not see how such wide planet-moon pairs can form around stars.

Starting with a enormous population of ($\gtrsim 10^4$) isolated free-floating planetary mass objects among the stars would grossly overproduce the expected number of free floaters, which is not observed, and still fails to reproduce the observed number of JuMBOs. This model, however, naturally leads to a mass-ratio distribution skewed to unity, as is observed. We consider this model undesireable by the lack of a large ($\gtrsim 10^4$) population of free floating planets in the Trapezium cluster.

Ruling out models $\mathcal{SPP}$, $\mathcal{SPM}$ and $\mathcal{FFC}$, we are left with the simplest and most satisfactory solution in which JuMBOs form together with the single stars in the cluster. This model does not only reproduce the observed rates, it can subsequently also be used to further constrain the initial conditions of JuMBOs.

In the Plummer models, 80% of JuMBOs are ionized within 1 Myr. The observed population of free floaters and JuMBOs can then be reproduced if the cluster was born with some 500 free floating jupiter-mass planets and $\sim$ 50 JuMBOs. The current observed primary and secondary masses of JuMBOs would then still reflect the conditions at birth, but the semi-major axis and eccentricity distributions would have been affected by encounters with other cluster members. These processes tend to drive the eccentricity distribution to resemble the thermal distribution (probably with an excess of high ($\gtrsim 0.8$) eccentricities [**?**]. The semi-major axes of the jumbos would have widened, on average by approximately 5% due to encounters with other cluster members (mainly stars and free-floating planets).

Alternative to a Plummer initial stellar distribution we experimented with fractal distributions, which also satisfactorily reproduces the observed populations. In the fractal models, $\sim$ 90 % of the priordial JuMBOs become ionized, and in principle the entire observed populations of free-floating jupiter mass objects and JuMBOs can be explained by a single population of primordial JuMBOs. We then conclude that single jupiter mass objects are preferentially born in pars with a rather flat distribution in orbital separations with a maximum of about 100 au or 200 au.

This model satisfactorily explains the observed orbital separation distribution, with a $\sim$ 15% excess of systems with a separation $\gtrsim$ 400 au. We do expect a rich population of orbits with separation smaller than the observed 25 au, possibly down to sub-au scales. The masses of the primaries in the planet pairs, and the mass-ratio distribution are then hardly affected by the past $\sim$ 1 Myr evolution of the Trapezium cluster.

We have a slight preference for the $\mathcal{ISF}$ fractal models with 0.5 pc virial radius because hierarchical triple planets form naturally in roughly the observed proportion (on average 4 triples among $\sim$ 40 pairs and $\sim$ 500 single planets). The singles then originate from broken up pairs, and the trples form in interactions between two planet pairs. The dynamical formation of soft triple planets is quite remarkable, and observational follow-up would be of considerable interest.

Are they planets, or gaseous fuzzballs?

formed late if fractal

[10] argued that JuMBOs potentially originate from tilted circum-binary planets. Formed as a –sort-of– planet-moon system in a wide orbit around a star, that is strippied from the host star by the cluster potential or a relatively wide encounter with another star.

Single free floating planetary objects were discovered in abundance (between 70 and 170 candidates) before in the Upper Scorpius association [5], but these were considered to be single free floaters. With an age of about 11 Myr [**?**], Upper Scorpio is expected to be rich in single jupiter mass free floating planets, but binaries will be rare as these have been broken.

The orbital parameters of the JuMBOs hardly seem to depend on the cluster density (or virial radius). We do expect some difference in the JuMBO population as a fuction of the initial cluster

density, but the distribution JuMBO parameters are wide and they probaby do not form the right population to make such a distinction.

Software used for this study

In this work we used the following packages: `python` [**?**, **?**], `SeBa` [**?**, **?**], `AMUSE` [39], `numpy` [**?**], `scipy` [42], `sklearn` [**?**], `matplotlib` [**?**], and `sqlite3`.

Energy Consumption

The 820 simulations conducted during this investigation had a total wall-clock time of 432 days. For the XYZ runs, each CPU used 6 cores, for the other two configurations 18 cores were used per CPU. In total, the CPU time for all simulations was 7680 days. Assuming a CPU consumption rate of 12 Watt hr^{-1} [**?**], the total energy consumption is roughly 2210 kWh. For an emission intensity of 0.283 kWh kg^{-1} [**?**], our calculations emitted 7.8 tonnes of CO2, roughly equivalent to two round trips by plane New York - Beijing.

Acknowledgments

Veronica Saz Ulibarrena, Shuo Huang, Maite Wilhelm, Brent Maas, Fred Rasio, Alvaro Hacar.

References

[1] S. G. Pearson and M. J. McCaughrean, *Jupiter Mass Binary Objects in the Trapezium Cluster*, arXiv e-prints arXiv:2310.01231 (2023), doi:10.48550/arXiv.2310.01231, `2310.01231`.

[2] M. R. Zapatero Osorio, V. J. S. Béjar, E. L. Martín, R. Rebolo, D. Barrado y Navascués, C. A. L. Bailer-Jones and R. Mundt, *Discovery of Young, Isolated Planetary Mass Objects in the σ Orionis Star Cluster*, Science **290**(5489), 103 (2000), doi:10.1126/science.290.5489.103.

[3] P. W. Lucas and P. F. Roche, *A population of very young brown dwarfs and free-floating planets in Orion*, MNRAS **314**, 858 (2000), doi:10.1046/j.1365-8711.2000.03515.x, `arXiv:astro-ph/0003061`.

[4] R. Mundt, C. A. L. Bailer-Jones, M. R. Zapatero Osorio, V. J. S. Béjar, R. Rebolo, D. Barrado Y Navascués and E. L. Martin, *Discovery of Very Young Free-floating Giant Planets in the σ Orionis Cluster*, In *Astronomische Gesellschaft Meeting Abstracts*, vol. 17 of *Astronomische Gesellschaft Meeting Abstracts* (2000).

[5] N. Miret-Roig, H. Bouy, S. N. Raymond, M. Tamura, E. Bertin, D. Barrado, J. Olivares, P. A. B. Galli, J.-C. Cuillandre, L. M. Sarro, A. Berihuete and N. Huélamo, *A rich population of free-floating planets in the Upper Scorpius young stellar association*, Nature Astronomy **6**, 89 (2022), doi:10.1038/s41550-021-01513-x, `2112.11999`.

[6] T. Sumi, K. Kamiya, D. P. Bennett, I. A. Bond, F. Abe, C. S. Botzler, A. Fukui, K. Furusawa, J. B. Hearnshaw, Y. Itow, P. M. Kilmartin, A. Korpela *et al.*, *Unbound or distant*

planetary mass population detected by gravitational microlensing, Nat **473**, 349 (2011), doi:10.1038/nature10092, 1105.3544.

[7] N. Miret-Roig, *The origin of free-floating planets*, Ap&SS **368**(3), 17 (2023), doi:10.1007/s10509-023-04175-5, 2303.05522.

[8] C. Low and D. Lynden-Bell, *The minimum Jeans mass or when fragmentation must stop.*, MNRAS **176**, 367 (1976), doi:10.1093/mnras/176.2.367.

[9] D. F. A. Boyd and A. P. Whitworth, *The minimum mass for opacity-limited fragmentation in turbulent cloud cores*, A&A **430**, 1059 (2005), doi:10.1051/0004-6361:20041703, astro-ph/0411495.

[10] C. Chen, R. G. Martin, S. H. Lubow and C. J. Nixon, *Tilted circumbinary planetary systems as efficient progenitors of free-floating planets*, arXiv e-prints arXiv:2310.15603 (2023), 2310.15603.

[11] A. van Elteren, S. Portegies Zwart, I. Pelupessy, M. X. Cai and S. L. W. McMillan, *Survivability of planetary systems in young and dense star clusters*, A&A **624**, A120 (2019), doi:10.1051/0004-6361/201834641, 1902.04652.

[12] F. A. Rasio and E. B. Ford, *Dynamical instabilities and the formation of extrasolar planetary systems*, Science **274**, 954 (1996), doi:10.1126/science.274.5289.954.

[13] X. Zheng, M. B. N. Kouwenhoven and L. Wang, *The dynamical fate of planetary systems in young star clusters*, MNRAS **453**, 2759 (2015), doi:10.1093/mnras/stv1832, 1508.01593.

[14] J. R. Hurley and M. M. Shara, *Free-floating Planets in Stellar Clusters: Not So Surprising*, ApJ **565**, 1251 (2002), doi:10.1086/337921, astro-ph/0108350.

[15] M. X. Cai, M. B. N. Kouwenhoven, S. F. Portegies Zwart and R. Spurzem, *Stability of multi-planetary systems in star clusters*, MNRAS **470**, 4337 (2017), doi:10.1093/mnras/stx1464, 1706.03789.

[16] F. Flammini Dotti, M. B. N. Kouwenhoven, M. X. Cai and R. Spurzem, *Planetary systems in a star cluster I: the Solar system scenario*, MNRAS **489**(2), 2280 (2019), doi:10.1093/mnras/stz2346, 1908.07747.

[17] E. B. Ford, M. Havlickova and F. A. Rasio, *Dynamical Instabilities in Extrasolar Planetary Systems Containing Two Giant Planets*, Icarus **150**(2), 303 (2001), doi:10.1006/icar.2001.6588, astro-ph/0010178.

[18] W. Hao, M. B. N. Kouwenhoven and R. Spurzem, *The dynamical evolution of multiplanet systems in open clusters*, MNRAS **433**, 867 (2013), doi:10.1093/mnras/stt771, 1305.1413.

[19] K. Stock, M. X. Cai, R. Spurzem, M. B. N. Kouwenhoven and S. Portegies Zwart, *On the survival of resonant and non-resonant planetary systems in star clusters*, MNRAS **497**(2), 1807 (2020), doi:10.1093/mnras/staa2047, 2007.11601.

[20] J. D. Kirkpatrick, C. R. Gelino, J. K. Faherty, A. M. Meisner, D. Caselden, A. C. Schneider, F. Marocco, A. J. Cayago, R. L. Smart, P. R. Eisenhardt, M. J. Kuchner, E. L. Wright *et al.*, *The Field Substellar Mass Function Based on the Full-sky 20 pc Census of 525 L, T, and Y Dwarfs*, ApJS **253**(1), 7 (2021), doi:10.3847/1538-4365/abd107, 2011.11616.

[21] W. M. J. Best, M. C. Liu, T. J. Dupuy and E. A. Magnier, *The Young L Dwarf 2MASS J11193254-1137466 Is a Planetary-mass Binary*, ApJL **843**(1), L4 (2017), doi:10.3847/2041-8213/aa76df, 1706.01883.

[22] C. Beichman, C. R. Gelino, J. D. Kirkpatrick, T. S. Barman, K. A. Marsh, M. C. Cushing and E. L. Wright, *The Coldest Brown Dwarf (or Free-floating Planet)?: The Y Dwarf WISE 1828+2650*, ApJ **764**(1), 101 (2013), doi:10.1088/0004-637X/764/1/101, 1301.1669.

[23] P. Calissendorff, M. De Furio, M. Meyer, L. Albert, C. Aganze, M. Ali-Dib, D. C. Bardalez Gagliuffi, F. Baron, C. A. Beichman, A. J. Burgasser, M. C. Cushing, J. K. Faherty *et al.*, *JWST/NIRCam Discovery of the First Y+Y Brown Dwarf Binary: WISE J033605.05-014350.4*, ApJL **947**(2), L30 (2023), doi:10.3847/2041-8213/acc86d, 2303.16923.

[24] K. Kellogg, S. Metchev, P. A. Miles-Páez and M. E. Tannock, *A Statistical Survey of Peculiar L and T Dwarfs in SDSS, 2MASS, and WISE*, AJ **154**(3), 112 (2017), doi:10.3847/1538-3881/aa83b0, 1708.03688.

[25] S. C. Eriksson, M. Janson and P. Calissendorff, *Detection of new strongly variable brown dwarfs in the L/T transition*, A&A **629**, A145 (2019), doi:10.1051/0004-6361/201935671, 1910.02638.

[26] C. Clanton and B. S. Gaudi, *Synthesizing Exoplanet Demographics: A Single Population of Long-period Planetary Companions to M Dwarfs Consistent with Microlensing, Radial Velocity, and Direct Imaging Surveys*, ApJ **819**(2), 125 (2016), doi:10.3847/0004-637X/819/2/125, 1508.04434.

[27] Y. Wang, R. Perna and Z. Zhu, *Floating binary planets from ejections during close stellar encounters*, arXiv e-prints arXiv:2310.06016 (2023), doi:10.48550/arXiv.2310.06016, 2310.06016.

[28] M. B. N. Kouwenhoven, S. P. Goodwin, R. J. Parker, M. B. Davies, D. Malmberg and P. Kroupa, *The formation of very wide binaries during the star cluster dissolution phase*, MNRAS **404**(4), 1835 (2010), doi:10.1111/j.1365-2966.2010.16399.x, 1001.3969.

[29] H. B. Perets and M. B. N. Kouwenhoven, *On the Origin of Planets at Very Wide Orbits from the Recapture of Free Floating Planets*, ApJ **750**, 83 (2012), doi:10.1088/0004-637X/750/1/83, 1202.2362.

[30] N. Goulinski and E. N. Ribak, *Capture of free-floating planets by planetary systems*, MNRAS **473**(2), 1589 (2018), doi:10.1093/mnras/stx2506, 1705.10332.

[31] S. F. Portegies Zwart, *Stellar disc destruction by dynamical interactions in the Orion Trapezium star cluster*, MNRAS **457**, 313 (2016), doi:10.1093/mnras/stv2831, 1511.08900.

[32] H. C. Plummer, *On the problem of distribution in globular star clusters*, MNRAS **71**, 460 (1911).

[33] D. C. Heggie, *Binary evolution in stellar dynamics*, MNRAS **173**, 729 (1975).

[34] P. Kroupa, *The Initial Mass Function of Stars: Evidence for Uniformity in Variable Systems*, Science **295**, 82 (2002), doi:10.1126/science.1067524, arXiv:astro-ph/0201098.

[35] T. Sumi, N. Koshimoto, D. P. Bennett, N. J. Rattenbury, F. Abe, R. Barry, A. Bhattacharya, I. A. Bond, H. Fujii, A. Fukui, R. Hamada, Y. Hirao *et al.*, *Free-floating Planet Mass Function from MOA-II 9 yr Survey toward the Galactic Bulge*, AJ **166**(3), 108 (2023), doi:10.3847/1538-3881/ace688, 2303.08280.

[36] S. F. Portegies Zwart, T. C. N. Boekholt, E. H. Por, A. S. Hamers and S. L. W. McMillan, *Chaos in self-gravitating many-body systems. Lyapunov time dependence of N and the influence of general relativity*, A&A **659**, A86 (2022), doi:10.1051/0004-6361/202141789, 2109.11012.

[37] S. Portegies Zwart, S. L. W. McMillan, E. van Elteren, I. Pelupessy and N. de Vries, *Multi-physics simulations using a hierarchical interchangeable software interface*, Computer Physics Communications **183**, 456 (2013), doi:http://dx.doi.org/10.1016/j.cpc.2012.09.024, 1204.5522.

[38] F. I. Pelupessy, A. van Elteren, N. de Vries, S. L. W. McMillan, N. Drost and S. F. Portegies Zwart, *The Astrophysical Multipurpose Software Environment*, A&A **557**, A84 (2013), doi:10.1051/0004-6361/201321252, 1307.3016.

[39] S. Portegies Zwart and S. McMillan, *Astrophysical Recipes; The art of AMUSE*, doi:10.1088/978-0-7503-1320-9 (2018).

[40] S. Portegies Zwart and T. Boekholt, *On the minimal accuracy required for simulating self-gravitating systems by means of direct n-body methods*, The Astrophysical Journal Letters **785**(1), L3 (2014).

[41] S. M. Vicente and J. Alves, *Size distribution of circumstellar disks in the Trapezium cluster*, A&A **441**, 195 (2005), doi:10.1051/0004-6361:20053540, astro-ph/0506585.

[42] E. Jones, T. Oliphant, P. Peterson *et al.*, *SciPy: Open source scientific tools for Python* (2001–).

A Similarity between r_{ij} and a

The comparison between simulations and observations is somewhat hindered by the different perspecitves. Whereas dynamicists prefer to use Kepler orbital elements, from an observational perspective such data is not always available. In our current study, we try to compare populations of binaries with observed objects. The latter are projected separattions, which do not directly translate in orbital elements without full knowledge of the 6-dimension phase space of the orbit. We thereofre have to compare projects separation with what we prefer to use, the semi-major axis of a bound two body orbit.

Figures 14 and 15 motivate our choice of analysing results in terms of the semi-major axis given the similarity between the curves.

In all cases, r_{ij} exhibits longer tails at the detriment of the shorter separations/orbits. However, these differences are so small - especially in the Fractal case for which most of our discussion revolves around - that we can safely interchange between one and the other. In doing so, we assume that the observed projected separation of JuMBOs are equivalent to their semi-major axis, easing our discussion.

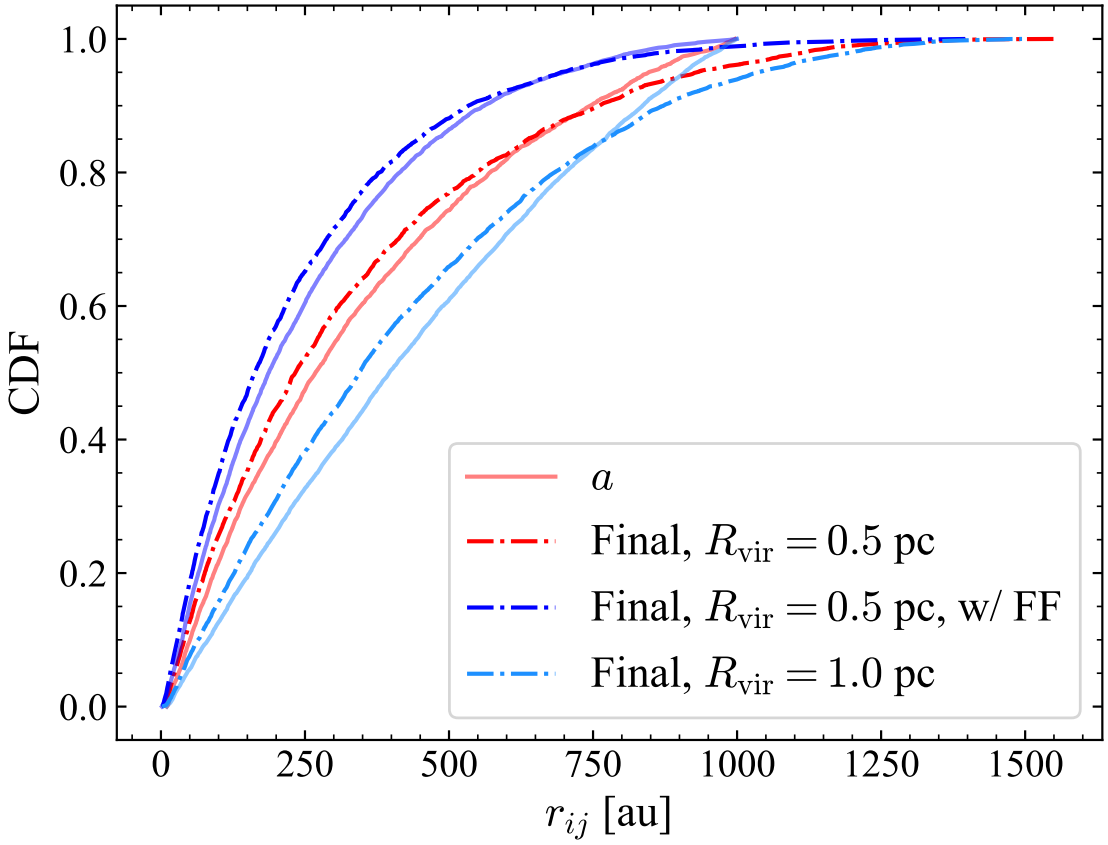

Figure 14: CDF of surviving JuMBO projected separation distribution for models P05, P05FF, P1. Overplotted are translucent lines denoting the respective models' JuMBOs semi-major axis.

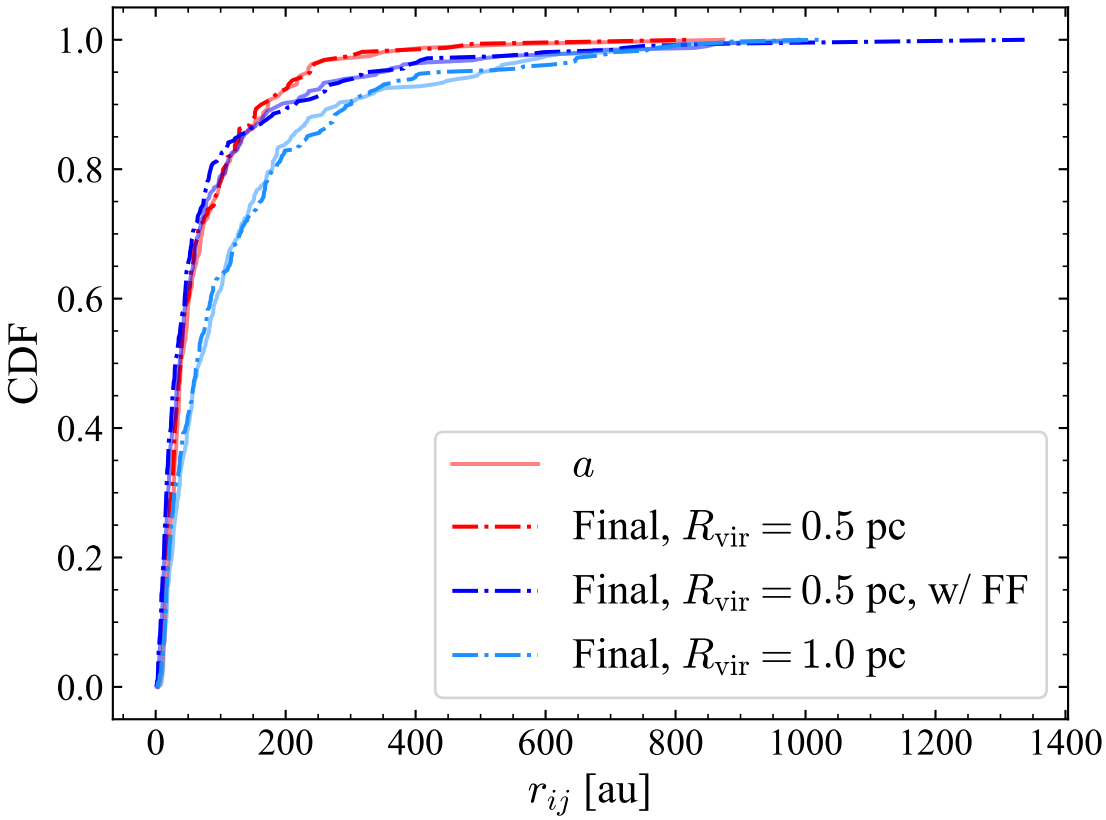

Figure 15: CDF of surviving JuMBO projected separation distribution for models F05, F05FF, F1. Overplotted are translucent lines denoting the respective models' JuMBOs semi-major axis.